Marble wastes recycling: Design and synthesis of low-temperature calcium silicate hydrate under various CaO:SiO2 ratio and alkalinity

Marble Wastes Recycling: Design and Synthesis of low-temperature Calcium Silicate Hydrate under various $CaO:SiO_2$ ratio and alkalinity

Elie Kamseu[1,2*], Valeria Alzari[1], Roberto Rosa[3], Daniele Nuvoli[1], Davide Sanna[1], Alberto Mariani[1], Cristina Leonelli[2]

[1]Dipartimento di Chimica e Farmacia, Università di Sassari, and INSTM, Via Vienna 2, 07100 Sassari, Italy

[2]Department of Engineering "Enzo Ferrari", University of Modena and Reggio Emilia, Via Pietro Vivarelli 10, 41125 Modena, Italy

[3]University of Modena and Reggio Emilia, Department of Sciences and Methods for Engineering, Via Amendola 2, 42122 Reggio Emilia , Italy

Abstract: Marble sludge wastes (MSW) are investigated as solid precursor for the production of low-temperature calcium silicate hydrate (CSH). Calcined powder of MSW is ball-milled with rice husk ash (RHA) and the slurries are treated in oven at 100C for 24 hours in a context where water evaporation is minimized. The initial CaO: SiO_2 molar ratio varies from 1 to 3 (CS, C_2S and C_3S) and the solution used for the preparation of the calcium silicate hydrate presents NaOH with concentration of 0, 1, 2 and 3 N. FTIR, XRD, Particle size distribution, BET surface area and Environmental Scanning Electron Microscope (ESEM) permitted to confirm the formation of C_xS (x = 1, 2, 3) and CSH at 100℃ through pozzolanic reactions. The increase of the alkalinity of the solution improved the silica dissolution and enhances the formation of C_xS and CSH up to 2N. Further increase of the alkalinity affected the silica polymerization, the particle size and the concentration of C_xS and CSH into the final matrix. Precursor with $CaO:SiO_2$ = 1 seem to promote more monomers while $2CaO:SiO_2$ and 3CaO:SiO2 resulted in orthosilicate chains and interlayer respectively. The high reactivity and fine particles (ϕ < 32 nm) of CSH obtained appeared promising for the design of low-cost, environmentally-friendly and sustainable binders as well as others engineering applications including refractory precursors, hydroceramics, insulating matrices, filtration and catalysis.

Key words: Marble sludge waste, recycling, calcium silicate hydrate, sustainable binder.

*Corresponding author: Email: kamseuelie2001@yahoo.fr; Tel: 0039079229528

1. Introductiom

According to Marmo News, 2018, the gradient of growth regarding the World's production of Marble and dimension Stones is more important than that of the World's economy when considering the period from 1998 to 2018. During this period the total volume of production moved from 51 x 10^6 kgs to 153 x 10^6 kgs. Applying the theory of the 75 vol.% of wastes during the production cycle of Marble and dimension stones in industries, it can be concluded that in 20 years, 459 x 10^6 kgs of wastes have been produced in the sector. This represents 1.83 wt.% of the industrial solid wastes produced Worldwide. Considering that Marble and dimension stone wastes are not biodegradable, the preoccupation of Traverso et al. 2010 [1], remains actual and need particular attention. Solutions that appear into the literature propose the integration of the wastes into concretes as for the replacement of cement and aggregates [2, 3]. The chemical and mineralogical characterization present marble wastes as made from $CaCO_3$ (> 80 wt.%) with the principal mineral being calcite. The waste are then alkali-reactive [4, 5, 6] means that their introduction into the concrete matrices has significant limits. Fine particles should not be applied at more than 10 wt.% in concretes. It is therefore important to find new solutions for the recycling and management of waste marbles. Proposing recycling processes that take into account the protection of the environment and the recycling of wastes to useful products sound more promising and sustainable for the World's future development.

In the region of sardaigne in Italy, one of the important pole of marble production, the industries share the geographic area with the producers of biomas, Rice Husk Ash (RHA), which is made essentially of SiO_2 (> 90 wt%). Both wastes constitute serious environmentally and ecological problems for the region and country. Wastes marble will decompose to highy reactive CaO during calcination at 800-850°C. CaO as $Ca(OH)_2$ will react with the SiO_2 to form Calcium silicate and Calcium Silicate Hydrate (CSH). This can take place through pozzolanic reactions at room temperature with a long time scale. Homogeneous nucleation has been described for the production of CSH in the supersaturate solution with various Ca/Si molar ratios. Ca/Si ratios under 0.1 allow sponaneous nucleation with homogeneous nucleids. The induction time is less than 20 min [7]. The increase of the Ca/Si affects the nucleation and formation of homogeneous nucleids of CSH. However, the application of the temperature as lower as 150°C allows to improve the homogeneous nucleation and significantly reduce the formation time [8]. The nucleation of CSH from lime and silica is described as homogeneous nucleation compared to CSH from the cement hydration. Nonat, 1999 [7], showed that direct nucleation have time of induction as fast as 20 min according to the $CaO:SiO_2$ molar ratio. The CSH growth proceeds by agglomeration of nanometric thin elements.

Lime concentration in solution controls the rate of agglomeration: the lower the lime concentration the faster CSH grows [7,9]. The production of low-temperature calcium silicate hydrate appears nowadays as alternative ecological, low-energy and sustainable binder [7, 17]. CSH can be directly used or calcined at relatively low temperature (900-1000°C) for the production of belite [4, 10] that will be directly hydrated to binding phases useful in the area of structural matrices or applied as refractories, heat resistant coating, bioactive self-setting .materials and electrical insulators [4, 10].
The objective of this research is to propose local solution for an intensive valorisation of the marble and RHA by developing sustainable process in which alkaline solution is used to improve the CSH nucleation and maintain the temperature of the nucleation under 100°C in a pozzolanic reaction context using ordinary equipments. The range of Ca/Si, the most stable calcium silicate hydrate is considered and the effects of calcium concentration as well as level of alkalinity are used to investigate the feasibility of our objectives.

2. Materials and Methods

2.1 Materials

The pozzolanic synthesis of calcium silicate hydrate involved two industrial wastes from the region of Sardaigne in Italy. The fine powder recycled from the production of marble and Rice Husk Ash (RHA) from the agricultural industry. Figure 1a shows the XRD patterns of the Marble and RHA. The powder of marble appears to be essentially calcite while the RHA presents high amount of amorphous silica illustrated with the hump between 25 and 30̊ 2θ (Figure 1b). The thermal behaviour of the marble as showed into the Figure 2 lets observe the decomposition of the calcite contained into the marble at 820-840°C: 32 wt% of weight loss is identified confirming the presence of impurities of silica nature as showed with XRD patterns in Figure 1a. The CaO ($Ca(OH)_2$ was prepared by calcination of the powder of marble at 825 for 4 hours: 5°C/min with a soaking time of 75 min at maximum temperature. The analysis of the powder shown that the CaO which we stored into closed area was stabilized as $Ca(OH)_2$. The final powders of $Ca(OH)_2$ and amorphous RHA were having particle size under 32 um after grinding (ball-mill).

2.2 Synthesis of Calcium Silicate Hydrate (S-C-H)

The Calcium silicate Hydrate was prepared from pozzolanic reactions of amorphous silica (RHA) and $Ca(OH)_2$ from calcined marble in solution with high liquid/solid ratio (> 3). The solution used for the preparation of the calcium silicate hydrate was aqueous NaOH at 0, 1, 2 and 3N. Stochiometric amounts of $Ca(OH)_2$ and SiO_2 were prepared and mixed to have three different grades of calcium silicates: $CaO:SiO_2$ (CS), $2CaO:SiO_2$ (C2S) and $3CaO:SiO_2$ (C3S). The mixes

were ball-milled in porcelain jar for 40 min using Rapid-Mill (MGS, Modena Italy) with rpm = 1200. The slurries obtained were cured still in an excess of water in closed Teflon tubes at the temperature of 100°C for 48h. In general the slurries remained with water in closed Teflon up to 48 hours and the semi-dried powders of calcium silicate hydrate are analysed immediately after synthesis, the Telflon tubes allowing the evaporation of water in a very slow rate. The synthetized powders are keeping in closed plastic to limit at maximum the carbonization. Finally the powders collected were CS, CS1N, CS2N and CS3N for the CS having $CaO:SiO_2$ = 1. C2S, C2S1N, C2S2N, C2S3N for $2CaO:SiO_2$ and C3S, C3S1N, C3S2N and C3S3N for $3CaO:SiO_2$.

2.3 Calcium Silicate hydrate characterization

The influence of the $CaO:SiO_2$ molar ratio and the alkalinity of the solution into the phases evolution was investigated with X-ray diffraction and FTIR infrared spectroscopy. Experiments were performed on a Panalytical copper Pro diffractomer (Bruker) with the RX tube using a copper anticathode ($\lambda K\alpha 1$ = 1.5405Å). The working condition of the diffractometer was 40 KV and 40 mA. The data were collected at the range from 5 to 70° 2θ using steps of 0.02° and measurement time equivalent to 0.02s per step. The detector was a Goniometer with geometry theta-theta. The 2θ diffraction patterns were analysed by the mean of EVA 21.0 software (Bruker). Since calcium silicate hydrates are poorly crystalline structures, the complexity of those matrices required more than X-ray diffraction to be elucidated. FT-IR spectroscopy is an analytical technique sensitive to vibrational modes. It is possible then to have detailed informations on the local atomic structure of CSH by measuring the vibrational modes. The data regarding the different molecular bonds are used to describe the structural morphology of the calcium silicate hydrate powders that were finely grounded prior to the analysed. The FT-IR spectra were collected by the mean of spectrophotometer NICOLET 6700 FTIR series. The range of the spectra collected were 4000 to 600 cm^{-1} and the spectra resolution 2 cm^{-1}.

The distribution of different phases (particles size) within each powder of calcium silicate hydrate were analysed with the MASTERSIZE 2000. The analytical method combine the Fraunhofer model and Mie theory using optical bench to capture the scattering pattern from the field of particles and calculating the particles size by the Malvern Software. The surface area has been defined (ISO 2012)[11] as quantity of accessible surface of a sample when exposed either to gaseous or liquid absorbate phase. It is determined based on Brunauer-Emmett-Teller (BET theory) which is based on the physical multilayers adsorption of non corrosive gases. The theory is the most common and standardized (ISO9277-2010; DIN 9277-2013) [12, 13] analysis method for the measurement of the specific surface area.

Freshly synthetized powders of calcium silicate hydrate were collected for micrographic and morphological observations. Fine powders are deposited into the sample holder (aluminum stap) which received initially the carbon liquid that allow to fix the particles of calcium silicate hydrate and drying. The specimens are gold coated (10 nm thickness) using a stupper working in high pressure. Microstructure observations are performed using an Environment Scanning Electron Microscope (ESEM, Quanta200, FEI). The analysis were done using functioning parameters working at 30 Kv and 30 mA.

3 Results

3.1 Phases characterization

Figure 3 shows the XRD patterns of semi-dried powders of the semi-dried powders of calcium silicate synthetized with different Ca/Si molar ratios (CS, C2S and C3S) as function of the NaOH concentration. The CSH powders from the pozzolanic synthesis at 100°C consist of a mix of CSH and anhydrous CS (β-C_2S and γ-C_2S). In fact large peaks overlap and large polymorphism coexistence of calcium silicate hydrate and calcium silicate anhydride make the phase identification challenging. The characteristics of CaO (2theta = 32.2 and 2 theta = 37.3) are absent into the XRD patterns or did not significant appear traducing the important degree of conversion of the mixes to calcium silicate phases. CS appear mostly in the CS serie is attributed to anhydrous calcium calcium silica. The amount of CS decreased (references to the peaks intensities) with the increase of NaOH concentration and more amorphous CSH is formed.

In the meantime β-C_2S and γ-C_2S are present. C_2S can exist in three different polymorphisms: α, β and γ. However, β-C_2S is the most usual and the evolution of the peaks of C_2S let suggest that γ-C_2S is not present in significant amount as the decrease in intensity of C_2S at NaOH concentration of 3N is linked to its dissolution. When the 2CaO:SiO_2 precursor is used, the amount of CS into the final matrix decreases significantly. The decrease is as significant as the concentration of NaOH increases (Figure 3a). The 2CaO:SiO_2 matrix is made essentially of CSH, β-C_2S and γ-C_2S. As in CaO:SiO_2 serie, the concentration of NaOH affects the crystallinity of the system with important decrease in Calcium silicate hydrate and calcium silicate anhydrite. Amorphous content increases with the increase of NaOH concentration. The matrix with 3CaO:SiO_2 appeared more amorphous with almost no CS. Phases identified were CSH, β-C_2S and γ-C_2S as well as C_3S. As for CS, the increase of the NaOH (above 2N) concentration affect negatively the crystallization of CSH as from In fact, some authors argued that the excess of Si in solution in the presence of NaOH or KOH (high alkalinity) contributes to increase the pH of the system and hinder the nucleation of C-S-H crystallite [14, 15]. Others have demonstrated that the increase of alkalinity could contribute to

increase the dissolution of C-S-H nucleids and grains. It is our suggestion that as from 3N, NaOH is capable to form with soluble silica the sodium silicate that contribute in an increase of the amorphous content.

The composite with the solid precursor of $3CaO:1SiO_2$ shown similar trend as $2CaO:1SiO_2$. More weak peaks of semi-crystallized C-S-H accompanied the amorphous, semi-crystalline, crystalline tobermorite. As already noted the level of crystallinity dropped as the peak $2\theta = 8°$ that observed with the specimen without and with NaOH 1N disappeared. The silicate source used was amorphous which signifies that the dissolution and polymerization of silica, one of the most important step of the formation of CSH (tobermorite and others), was effective in all the series. The similarity in C_2S and C_3S confirm the fact that poor development of CSH (tobermorite and others) and instead CS is linked to an excess of Si which would have effectively hindered the nucleation of CSH. The mean length of silicate chains in C-S-H increases as the Ca/Si ratio decreased. More silica conducts to the polymerization of silica that is not always transformed to tobermorite. Some authors even evidence that those earlier formed C-S-H, metastable polymerized chains, hinder the nucleation and growth of tobermorite [14, 16]. This explain the difference in synthesis with CS, C_2S and C_3S.

Typical FTIR spectra of calcium silicate hydrate synthetized with $CaO:SiO_2 = 1$ is illustrated into Figure 4 with the effects of the alkalinity on the phases evolution. Principals peaks identified are 3270, 1759, 1592, 1422, 932, 902, 812 and 654 cm^{-1}. The broad band with peak at 3270 cm^{-1} refers to the OH stretching region. Features provides information regarding the hydrogen environments. This region contains signal from all OH stretching vibrations in the calcium silicate hydrate synthetized; interlayer and surface (Si-OH, Ca-OH and H_2O). No free band of the portlandite frequency is observed means that the OH band is characteristics of SiOH and H_2O stretching are accompanied with the band about 600 cm^{-1}. The peak intensity of those bands increases with the molarity of the solution used. It can be explained by the importance of the depolymerisation of the silica chain with the increase of the NaOH concentration: the increase of the structural disorder that in turn increase the capacity of the calcium silicate hydrate to fix OH molecules at the interlayers. The absence of Ca-OH linkages and the fact the OH bands are larger, much broader and less resolved makes suggesting that the calcium silicate hydrate produced is similar to tobermorite as the OH behavior was similar for CS, C_2S and C_3S series. Those three series have a complex group of bands in the regions 600-1250 cm^{-1} which are due to the asymmetric and symmetric stretching vibrations of Si-O bands. The band at ~600 cm^{-1} is linked to the Si-O-Si bending vibrations. The principal peak appears at ~960 cm^{-1} for CS with no NaOH addition during the preparation. The band shifted to lower values (948, 940 and 938 cm^{-1}) when the preparation was done with 1, 2 and

3N NaOH solution, respectively. At NaOH of 3N, a peak at 902 cm^{-1} appeared. The peak at ~960 cm^{-1} is linked to the Si-O stretching corresponding to the O-$SiCa_x$, O-Si_2 bonds developed during the formation of calcium silicate hydrate. While that of 902 cm^{-1} is particularly attributed to the O-$SiCa_x$ bonds. In the C_3S series, the principal peak of Si-O stretching appears at 1002 $cm^{-1}$and shifts to 972 cm^{-1} with 1N solution (NaOH) then decreases to 947 and 944 cm^{-1} respectively for 2 and 3N. The peak at 660 cm^{-1} remains at ~622, 660 for 1 and 2N and 666 cm^{-1} for 3N. the principal peak of Si-O stretching remains at 947 and 944 cm^{-1} respectively for 2 and 3N. The peak at 960-900 cm^{-1} that appears in all series is characteristic to the CSH phase of tobermorite (11Å and 14Å), jennite and C-S-H; that at 670 cm^{-1} is attributed to Si-O-Si bending modes of water that can be found in jennite and tobermorite. Between 800 and 1200 cm^{-1} the experimental spectrum shows a single broad feature made of a main peak just below 1000 $cm^{-1}$and some shoulders distributed in both sides of the broad peak (principal). The broadening nature of the region of the O-Si-Ca_x and O-SiO_2 (800-1200 cm^{-1}) is linked in some extend to the degree of structural disorder, as absence or displaced Si tetrahedral in the silicate chains due to the integration of Ca as the depolymerization of Si-O-Si and repolymerization of O-Si-Ca_x. On the high frequency of the principal peak, shoulder below 1100 cm^{-1} and bum around 1200 cm^{-1} are associated respectively to the stretching modes within chains (tobermorite, 14 Å) and tobermorite 11 Å. Both indicating the existence of double silicate chains. The 1200 cm^{-1} are specific to C_2S and C_3S without addition of NaOH (Figure 4) illustrating the difference of the level of silicate polymerization when the NaOH is used.

In all the CS, C_2S and C_3S series of calcium silicate produced, carbonization was effective and it was not possible to have specimen without the peak of CO_3^{2-} at ~1450 cm^{-1}. According to the storage time weak shoulder could also being observed at ~875 cm^{-1}. Peak that progressively increases in intensity with time as detailed described by Wang et al. 2019 (Wang et al., 2019). The intensity of the carbonation was found to vary being more important with C_3S and C_2S compared to CS. The concentration of the NaOH used also favours the rate of carbonization.

In the Figures 4 and 5, the peak at 1650 cm^{-1}decrease in intensity relatively with the increase of NaOH. In fact, the peak at 875 cm^{-1} that appears with calcium silicate hydrate without NaOH decrease in intensity with the increase of NaOH concentration as the result of the increase in polymerization and the reduction of unreacted phases particularly the $Ca(OH)_2$. The absence of the peaks at 712-713 cm^{-1} suggested the high reactivity during the formation of calcium silicate hydrate and the absence of calcite into the microstructure of CSH at earlier stage, particularly when NaOH is used.

3.2 Particle size distribution and BET surface area

Figure 6 shows the particle size distribution of the powders of calcium silicate hydrate (CSH) as function of the NaOH concentration. It is observed the difference in particle sizes with the $CaO:SiO_2$ molar ratio. With no addition of NaOH, the particle size distribution of CS shows a bimodal band of particles suggesting finer and coarse calcium silicates formed. The coarse particles are surely mixed with the remaining unreacted silica particles or coarsening polymerized silica. Increasing the $CaO:SiO_2$ molar ratio towards CS, C_2S and C_3S series, the second band (mode) decreased in intensity as the concentration of the silica decreased. The hypothesis of the silica polymerization that hinder the pozzolanic reactions for the formation of calcium silicate hydrates is postulated: coarsening Calcium Silicate anhydrite. Since the calcium silicate formed in these conditions is generally finer, the difference between their grains and polymerized silica is pronounced. Applying the NaOH at 1N, the concentration of coarses particles dropped. The particles with size under 10 µm increase in CS from 66.95 vol.% to 70.87 vol.% as the results of the action of the alkalinity during the dissolution process of silica that makes the d(0.1) dropped from 1.194 µm to 1.102 µm and d(0.5) from 5.705 µm to 4.788 µm. In the C2S serie, the action of NaOH at 1N makes the particle size distribution having a perfect monomodal band with coarses particles almost absent as the particles with size under 10 µm reached 93.17 vol.%. Similar trend is observed with C_3S when the concentration of NaOH reached 2N while the band for C_2S 2N increase the size although the perfect monomodal character. The d(0.1) in C_3S serie decrease from 1.229 µm at 0N to 1.04 µm and 0.921 µm respectively for 1N and 2N in the meantime the d(0.5) decrease; from 5.169 to 3.701 mm (1N) and 2.843 µm (2N). The concentration of particles finer than 10 µm increased from 66.98 for CS to 89.09 vol.% and dropped to 76.23 vol.% for C_2S and C_3S. The use of NaOH 1N make the particles under 10 µm increase in CS to 73.75 vol.% and even reached 93.15 vol.% in C2S and 85.71 vol.% in C3S. Increasing the alkalinity to 2N, the volume of particles under 10 µm was stabilized in CS at 72.80 vol.%, decreasing a little in C_2S (88.86 vol.%) while reaching the optimum with C_3S at 94.4 vol.%.

The length of calcium silicate chain is seem to be linked to the $CaO:SiO_2$ molar ratio of the starting materials. In fact it is generally demonstrated that, as seem with this study, nanostructure development of the CSH depends significantly to the silica skeleton evolution. When the silica is dominant (low calcium to silicate ratios), cluster evolution is dominated by the nucleation and growth of silica chains. Calcium atoms fill the cavities in the silicate deficient parts and the effects on the skeleton extension is very low: Network or branch structures are easily formed. With the CaO dominated the starting materials (high calcium to silicate ratio), the cluster aggregates process results from the combine of calcium ions and isolated silicate. From the low calcium/silicate to high

values, the calcium silicate hydrate evolved from amorphous to semi-crystalline or crystalline structure (ordered ellipsoid-like structure).

The coefficient of activity of the calcium silicate hydrate was affected by the $CaO:SiO_2$, the level of the dissolution of the silica as from the alkalinity of the solution used. It was also evidenced the reduction of the coefficient of activity of the calcium silicate hydrate with storage time. From the Figure 6, it is observed the coefficient of activity of CS series that increases with the increase of the NaOH concentration from 1 to 2N. When the concentration of NaOH reachs 3N the coefficient of activity of CS dropped under 1. This can be correlated to the particle size distribution while relatively coarse particles of calcium silicate are formed at 0N and fine particles can be optimized between 1 and 2N, before relative silica polymerization at 3N. At that level, potential formation of sodium silicate that reduces the C_{BET} is expected. Results in line with the FT-IR spectra with the optimal depolymerisation that takes place between 1 and 2N. Those conditions are very interesting for the formation of O-Si-Ca_x bonds: phases that surely increase the BET surface area and by the way the coefficient of activity of the calcium silicate hydrate prepared. After 28 days the C_{BET} of CS without NaOH decreased to 0.731, 0.755 and 0.79 respectively for 0, 1 and 2N. It is observed that with time the reduction of the coefficient of activity in the specimens with 3N (high potential of silica polymerization) is more pronounced compared to the specimens with 1 and 2N where the amount of NaOH does not significantly alter the microstructure. The reduction of the coefficient of activity is as important at 90 days of storage and the gap between the specimens with high NaOH concentration and others is significant. As significant as the concentration of silica is relatively high in CS, with high potential of non-reactive silica residue. Residue that favors the silica polymerization at high NaOH concentration. This explains the important resistance of the calcium silicate hydrate to the reduction of the coefficient of activity with the decrease in silica content in the series CS, C_2S and C_3S.

C_2S showed a C_{BET} that increases to 1.0918 and 1.049 when 1N and 2N NaOH solution are used. Values of C_{BET} slightly higher with regard to CS. The solution 3N reduced the C_{BET} only to 0.968 indicating a negligible effect with respect to CS at the same level of alkalinity. The storing time of 28 days and 90 days reduced the C_{BET} at 0.86 and 0.72 when 1N and 2N are used. The C_{BET} of 0.622 at 3N is very high with respect to the value of 0.12 in CS serie. C_3S serie shows a C_{BET} of 1.106, 1.107 and 1.024 respectively for 1, 2 and 3N. The tendency of the C_2S is confirmed with the reduction of the effects of Na ions even though the concentration of 3N is noted to affect the C_{BET} as correlated with the particles coarsening that is not positive for the reactivity of calcium silicate hydrate. The trend of the variation of the particles size and the coefficient of BET surface area in relation with the $CaO:SiO_2$ molar ratio can be interpreted with the hypothesis of the NaOH

(alkalinity) that acts as catalysis for the dissolution of silica particles and favors the nucleation and growth of calcium silicate hydrate (Gaggiano et al., 2013; Liu et al., 2019; Xia et al., 2019). In fact, unreacted particles of silica were found in significant amount into the matrix of CS with no NaOH addition. However, when the concentration of NaOH is above 2N, silica polymerization and formation of sodium silicate take place, hindering the nucleation and growth of calcium silicate hydrate. Moreover, the storing of the CS enhances the aggregation and formation of coarsening particles. Zhu et al [17] indicated that sodium ions can be absorbed at the surface and combine in the interlayer of CSH. In the presence of enough Ca, the polymerization of silica is reduced [18]. The effects of NaOH in the silica polymerization are directly linked to the concentration of silica with potential silica residue prompt to form sodium silica.

3.3 Microstructure

The micrographs of the Figure 8 present the morphology of calcium silicate influenced by the $CaO:SiO_2$ molar ratio. As already signified with XRD and FTIR patterns, the phases formed are also affected by the concentration of NaOH. CS series show homogeneous and dense agglomerations that are made from the particles of CS, C_2S in anhydrous and hydrous forms. The relatively high densification is linked to the long chains of silicate as the Ca/Si ~ 1 favors the formation of Calcium silicate hydrate with extended chains of silica polymerization. High magnification evidences aggregated particles with the light grey having relatively high Ca/Si while dark grey particles present relatively low Ca/Si. Those particles appear with globular-like structure having an extent of regularity in the size and distribution. In the C_2S specimens, the densification of the matrix decreases but the particle size decreases with higher range of homogeneity. The calcium silicate anhydrous and hydrates appear light and it is difficut to distinguish between hydrous and non hydrated phases. Mostly C_2S and C_3S phases are available. It is observed that the progressive increase of the $CaO:SiO_2$ molar ratio transforms the final calcium silicate from the globular to interlayered network.

It appears that the pozzolanic synthesis of calcium silicate hydrate results in the formation of Calcium Silicate Anhydrite (CS, β-C_2S, γ-C_2S, C-S-H including 11 and 14Å tobermorite as well as jennite-like structure. The used of NaOH modifies the level of polymerization and affect the silica chains present into the matrix. The layered structure of CSH increased from CS to C_3S confirming the data from the literature that confer to CSH monomeric structure for CS precursors, orthosilicate-like structure for CSH make from C_2S and more interlayers for CSH from C_3S.

4. Discussion and Conclusion

4.1 synthesis and characterization

Marble sludge wastes have virtually the same composition as the original marble stone and are considered as non-hazardous wastes; being made of 90 to 99 wt% of calcite ($CaCO_3$). Between 700 and 900℃, the calcite is decomposed to CaO, an high reactive grade of chemical oxydes [4]. Rice husk ash contains nearly 20 wt% of silica present in hydrated amorphous form. Controlled calcination will favour the production of amorphous silica having high reactivity, ultrafine size and large surface area. Due to their high pozzolanic activity, this rice husk ash silica finds applications among others (SiC, Si_3N_4, Ag_2Si, …) in high strength concretes and alternative raw materials for the production of CS and CSH, important component of the Portland cement. The presence of both silica and CaO solid precursors in the region of Sardaigne (Italy) gives sustainable idea for the promotion of locally sourced raw materials into the direction of low-cost, environmentally-friendly and low-energy binders for concretes, composites and others porous systems. CSH was successfully produced at low temperature and the effects of addition of NaOH as well as the $CaO:SiO_2$ molar ratio were showing with some possibilities of the optimization of the efficiency and sustainability in relation with the intrinsic performances of the final CS and CSH developed.

The FTIR spectra collected (Figures 3 and 4) showed a main spectral feature occurring between 600 and 1250 cm^{-1}. The almost unique and broad band instead of separed vibrational modes of Si-O-Si is significant for the chemical bonds present: disordered and consequently amorphous structure of CS and CSH. This amorphous structure is confirmed by the hump presents in all XRD patterns. So instead of sharp band of crystalline Si-O-Si, the broad band included that of Q^1, Q^2 and Q^3 corresponding to colloidal silica with size under 0.032 μm [19]. When the concentration of NaOH is low (N = 0 or 1), the Q^3 present at high NaOH concentraton disappears. The increase in the concentration of soluble silica conducted to the increase in polymerization of monomeric silicates that is enhanced with the increase in the concentration of NaOH (Figures 2, 3 and 4). The shoulder in the range 930-980 cm^{-1} (Figures 3 and 4) is indicative of the stretching vibration of Si-O-2NBO linkage (Q^2), that evidences two non-bridging oxygens. The band centered at 1060 cm^{-1} was observed essentially with specimens of CS and CSH in which no NaOH was added. This band is generally the expression of three overlapping stretching vibrations from Si-OH linkages, the siloxane bonds. Si-O-Si and the Si-O-NBO (Q^3): components linked to polymerized Si that is not formed in the presence of NaOH. The shift of the principal band (600-1250 cm^{-1}) of amorphous CS and CSH to lower frequencies as $CaO:SiO_2$ molar ratio increases is associated to the dissolution level of silica; formation of more complex species. The dissolution creates more surface area available for bonding of simple oligomer species and increases the proportion of silicon sites with

NBO[19]. The difference in silica dissolution and formation of CS and CSH phases directly affected the particles size distribution and the BET surface area as indicated into Figures 6 and 7. The mean particles size decreased with the increase of $CaO:SiO_2$ molar ratio. In the first time due to the poor dissolution of the silica species and at high concentration of NaOH; the polymerization of Si-O-Na affected the particles size. The role of the transformation of the microstructure of the CS and CSH with $CaO:SiO_2$ molar ratio (Figure 8) and the concentration of NaOH was confirmed with ESEM analysis as showng into Figure 8. The amorphous nature of silica that is responsible for the higher reactivity allowed, in high liquid/solid molar ratio, the homogeneity in the formation of CS and CSH with low residual species (Figure 8).

4.2 Potential applications

Calcium Silicates Hydrates (CSH) is the major hydration product of Portland Cement. CS and CSH have a wide range of chemical compositions: monsilicate can be produced with CS precursor and orthosilicate for C_2S while layered structure is achieved when C_3S is used. The structure of 14 Å-Tobermorite (equivalent to the CSH cement phase) is usually inferred from that of 11 Å-Tobermorite and its ideal chemical formula is $Ca_{2.25}[Si_3O_{7.5}(OH)_{1.5}] \cdot 8H_2O$. The primary structural unit of Tobermorite contains CaO polyhedral sheets sandwiched between single silicate chains. The silicate chains are based on a three units repeating pattern called *dreierketten* arrangement of 7.8 Å in length in which two of the tetrahedra point toward the CaO polyhedral sheet while the third points toward the interlayer void. These microstructural behaviors confer to calcium silicate hydrates binder properties as from their high BET surface area and fine particle size. They form the principal component of OPC cement and binders. Potential application into the areas of geopolymers and inorganic polymer cement includes enhances nucleation and growth of CASH phases and the reduction of the porosity conducing to the improvement of the densification and durability. They can be used to regulate the alkalinity of the inorganic polymer cement maintaining high mechanical performance.

Calcium silicate hydrate can acts as precursor for insulating foam for the building sector, especially the internal insulation of walls. It was proven that, due to the high capillary action and hydrothermal material properties, the foam can be used to improve the moisture protection, and the moisture control capacity. Additionally, the high pH inhibits the growth of fungus [14, 18, 20].

Calcium silicate hydrate has a very high selectivity for 2,2′-isomer, which is not obvious in the presence of acidic catalysts. The highest selectivity of 2,2′-isomer (94.67%) and yield (51.33%) for bisphenol were achieved over calcium silicate hydrate (Si/Ca = 3) catalyst at 383 K for 120 min. A

possible mechanism was proposed in accordance [21]. Changing the acidity and basicity of catalyst provides a way to improve the purity of isomers.

CSH possesses plenty of mesoporous structures with the pore size range of 3–20 nm. The maximum moisture adsorption capacity of CSH is very high. The superior humidity control performance of CS and CSH matrices can be attributed to the increase of specific surface area and pore volume and the more reasonable and uniform pore size distribution. Moreover, CSH also exhibits good reusability within cycles of adsorption/desorption. The moisture adsorption capacity of the coating matrix with CSH in 24 h at high humidity can reach 110 g/m^2, and the moisture desorption capacity can also reach 70 g/m^2 confirming the excellent humidity control performance of CSH matrix that can be used as a smart indoor humidity control material for various construction applications.

Calcium silicate hydrate has also proven to be potential candidates for biomedical applications because of their osteogenic properties. The conversion of CSH to calcium silicate powder resulting materials in medical applications for bone repair. The results indicated that the powder composition is dependent on the Ca:Si ratio of the precursors and on the sintering temperature. In addition, the setting times of the powder-derived cements were found to be independent of the sintering temperature and synthesis technique, but it was affected by the Ca:Si ratio of the precursors. The mechanical strength of the cements was similar. These encouraging results suggest that the hydrothermal method is a potentially beneficial alternative to the sol–gel route for the production of calcium silicate powders.

The fine particles size and high BET surface area make CS and CSH promising candidates for the ddensification and enhancing mechanical properties of geopolymers and inorganic polymer cement with nucleation/seeding and growth of CASH reinforcing CSH and NASH. The alternatives include also the transformation to porous (hydroceramics) ceramic and insulating matrices.

Conclusively, environmentally-friendly, sustainable and low-cost solutions have been proposed for the valorization of industrial wastes of the region of Sardaigne in Italy. The solution used locally sourced raw materials approach (wastes) and the cold-setting process. It was demonstrated that:

- Reactive grade of CaO and SiO_2 with fine particles size and high BET surface area can be produced from the marble sludge waste and RHA using appropriate thermal cycle.
- CaO and SiO_2 in aqueous (high liquid/solid ratio) solution produced a relatively low-temperature (100℃), various grade of SiO-OH bonds as results of the formation of Q^1, Q^2 and Q^3 species.
- The dissolution of silica and the formation of Si-O-Ca bonds permitted to evidence phases with characteristics similar to that of 11Å and 14Å tobermorite as well as jennite generally found in hydrated cement.

- The presence of tobermorite, jennite-like structures including β-C2S, γ-C2S, and CSH that dominated the CS, C2S and C3S matrices suggested successful transformation of the industrial wastes to potential new and sustainable precursors for various engineering and functional applications.

Acknowledgements: The authors of this paper wish to acknowledge the financial support of the Region of Sardegna, Italy.

References

[1]. Traverso, M., Rizzo, G., Finkbeiner, M., 2010. Environmental performance of building materials : life cycle assessment of a typical Sicilian marble 104–114. https://doi.org/10.1007/s11367-009-0135-z

[2]. Vardhan, K., Goyal, S., Siddique, R., Singh, M., 2015. Mechanical properties and microstructural analysis of cement mortar incorporating marble powder as partial replacement of cement. Constr. Build. Mater. 96, 615–621. https://doi.org/10.1016/j.conbuildmat.2015.08.071.

[3]. Ruiz-sánchez, A., Sánchez-polo, M., Rozalen, M., 2019. Waste marble dust : An interesting residue to produce cement 224, 99–108. https://doi.org/10.1016/j.conbuildmat.2019.07.031.

[4]. Maheswaran, S., Kalaiselvam, S., Karthikeyan, S.K.S.S., Kokila, C., Palani, G.S., 2016. β-belite cements (β-dicalcium silicate) obtained from calcined lime sludge and silica fume, Cement and Concrete Composites. Elsevier Ltd. https://doi.org/10.1016/j.cemconcomp.2015.11.008

[5]. L, Grangeon, S., Linard, Y., Chiaberge, C., 2013. X-ray diffraction : a powerful tool to probe and understand the structure of nanocrystalline calcium silicate hydrates. Acta Crystallogr B Struct Sci Cryst Eng Mater 15, 465–473. https://doi.org/10.1107/S2052519213021155.

[6]. Rodríguez, O., Frías, M., Rojas, M.I.S. De, 2008. INFLUENCE OF THE CALCINED PAPER SLUDGE ON THE DEVELOP- MENT OF HYDRATION HEAT IN BLENDED CEMENT MORTARS 92, 865–871.

[7]. Nonat, A., 1999. Experimental investigation of calcium silicate hydrate (C-S-H) nucleation 200, 565–574.

[8]. Rungchet, A., Poon, C.S., Chindaprasirt, P., Pimraksa, K., 2017. Synthesis of low-temperature calcium sulfoaluminate-belite cements from industrial wastes and their hydration : Comparative studies between lignite fl y ash and bottom ash. Cem. Concr. Compos. 83, 10–19. https://doi.org/10.1016/j.cemconcomp.2017.06.013.

[9]. Helene Viallis-Terrisse, A.N., 2001. Zeta-Potential Study of Calcium Silicate Hydrates Interacting with Alkaline Cations 65, 58–65. https://doi.org/10.1006/jcis.2001.7897.

[10]. Primus, C.M., Tay, F.R., Niu, L., 2019. Acta Biomaterialia Bioactive tri / dicalcium silicate cements for treatment of pulpal and periapical tissues. Acta Biomater. 96, 35–54. https://doi.org/10.1016/j.actbio.2019.05.050.

[11]. Marcelo L Garcia, Joana Sousa-Coutinho, Bernardino de Almeida, Roberto Frías, Peter A. Claisse, T.R.N., 2010. Grits as a Partial Cement Replacement for Concrete. Coventry Univ. andThe Univ. Wisconsin Milwaukee Cent. By-products Util. Int. Conf. Sustain. Constr. Mater. Technol. 28 □ June 30, 2010, Univ. Politec. delle Marche, Ancona, Italy.

[12]. ISO13317-4 2014 determination of the particle size distribution by gravitational liquid sedimentation methods-part 4: Balancemethod.

[13]. Liu, Y., Jia, H., Zhang, G., Sun, Z., Pan, Y., Zheng, S., 2019. Synthesis and humidity control performances of natural opoka based porous calcium silicate hydrate. Adv. Powder Technol. 30, 2733–2741. https://doi.org/10.1016/j.apt.2019.08.020.

[14]. Lognot, I., Klur, I., Nonae, A., 1998. NMR and Infrared Spectroscopies of C-S-H and AI-Substituted C-S-H Synthesised in Alkaline Solutions, Nuclear Magnetic Resonance Spectroscopy of Cement-Based Materials pp 189-196.

[15]. Zhu Ganyu, 2018. Synthesis of Calcium Silicate Hydrate in Highly Alkaline System. https://doi.org/10.1111/jace.14242.

[16]. Chen, J.J., Thomas, J.J., Taylor, H.F.W., Jennings, H.M., 2004. Solubility and structure of calcium silicate hydrate. Cem. Concr. Res. 34, 1499–1519. https://doi.org/10.1016/j.cemconres.2004.04.034.

[17]. Wang, D., Fang, Y., Zhang, Y., Chang, J., 2019. Changes in mineral composition , growth of calcite crystal , and promotion of physico-chemical properties induced by carbonation of β -C 2 S. J. CO2 Util. 34, 149–162. https://doi.org/10.1016/j.jcou.2019.06.005.

[18]. He, Y., Lu, L., Struble, L.J., Rapp, J.L., Mondal, P., 2013. Effect of calcium – silicon ratio on microstructure and nanostructure of calcium silicate hydrate synthesized by reaction of fumed silica and calcium oxide at room temperature. https://doi.org/10.1617/s11527-013-0062-0.

[19]. Gaggiano, R., Graeve, I. De, Mol, J.M.C., Verbeken, K., Kestens, L.A.I., 2013. An infrared spectroscopic study of sodium silicate adsorption on porous anodic alumina 1098–1104. https://doi.org/10.1002/sia.5230.

[20]. Matsushita, F., Aono, Y., Shibata, S., 2004. Calcium silicate structure and carbonation shrinkage of a tobermorite-based material 34, 1251–1257. https://doi.org/10.1016/j.cemconres.2003.12.016.

[21]. Xia, X., Xu, Y., Chen, Y., Liu, Y., Lu, Y., 2019. The distinct catalytic behaviours of calcium silicate hydrate for the high selectivity of 2 , 2 ′ -isomer in reaction of phenol with formaldehyde. Catal. Commun. 118, 15‑18. https://doi.org/10.1016/j.catcom.2018.09.004.

Figures and Tables Captions

Figure 1: XRD patterns of the raw industrial wastes: (a) Marble Sludge Waste; (b) Rice Husk Ash

Figure 2: Differential Thermal Analysis and Differential Thermal Gravimetric curves of marble sludge waste

Figure 3a: X-Ray Diffraction patterns of calcium silicate hydrate synthetized from CS solid precursor

Figure 3b: X-Ray Diffraction patterns of calcium silicate hydrate synthetized from C2S solid precursor

Figure 3c: X-Ray Diffraction patterns of calcium silicate hydrate synthetized from C3S solid precursor

Figure 4: Detailed FTIR spectra of the calcium silicate hydrate as function of the NaOH concentration showing the significant band of the calcium silicate hydrate in the range 800-1250 cm-1.

Figure 5a: Influence of the NaOH concentration on the broad band 800-1250 cm-1 in the calcium silicate hydrate synthetized with CS precursor

Figure 5b: Influence of the NaOH concentration on the broad band 800-1250 cm-1 in the calcium silicate hydrate synthetized with C2S precursor

Figure 5c: Influence of the NaOH concentration on the broad band 800-1250 cm-1 in the calcium silicate hydrate synthetized with C3S precursor

Figure 6a: Variation of the particle size distribution in the calcium silicate hydrate synthetized with CS precursor as function of the NaOH concentration

Figure 6b: Variation of the particle size distribution in the calcium silicate hydrate synthetized with C2S precursor as function of the NaOH concentration

Figure 6c: Variation of the particle size distribution in the calcium silicate hydrate synthetized with C3S precursor as function of the NaOH concentration

Figure 7a: Variation of the coefficient of the activity of the calcium silicate hydrate synthetized with CS as function of time (days)

Figure 7b: Variation of the coefficient of the activity of the calcium silicate hydrate synthetized with C2S as function of time (days)

Figure 7c: Variation of the coefficient of the activity of the calcium silicate hydrate synthetized with C3S as function of time (days)

Figure 8: Micrographs of the calcium silicate hydrate synthetized: (a) CS, (b) C2S, (c) C3S) and (d) C2S after carbonation

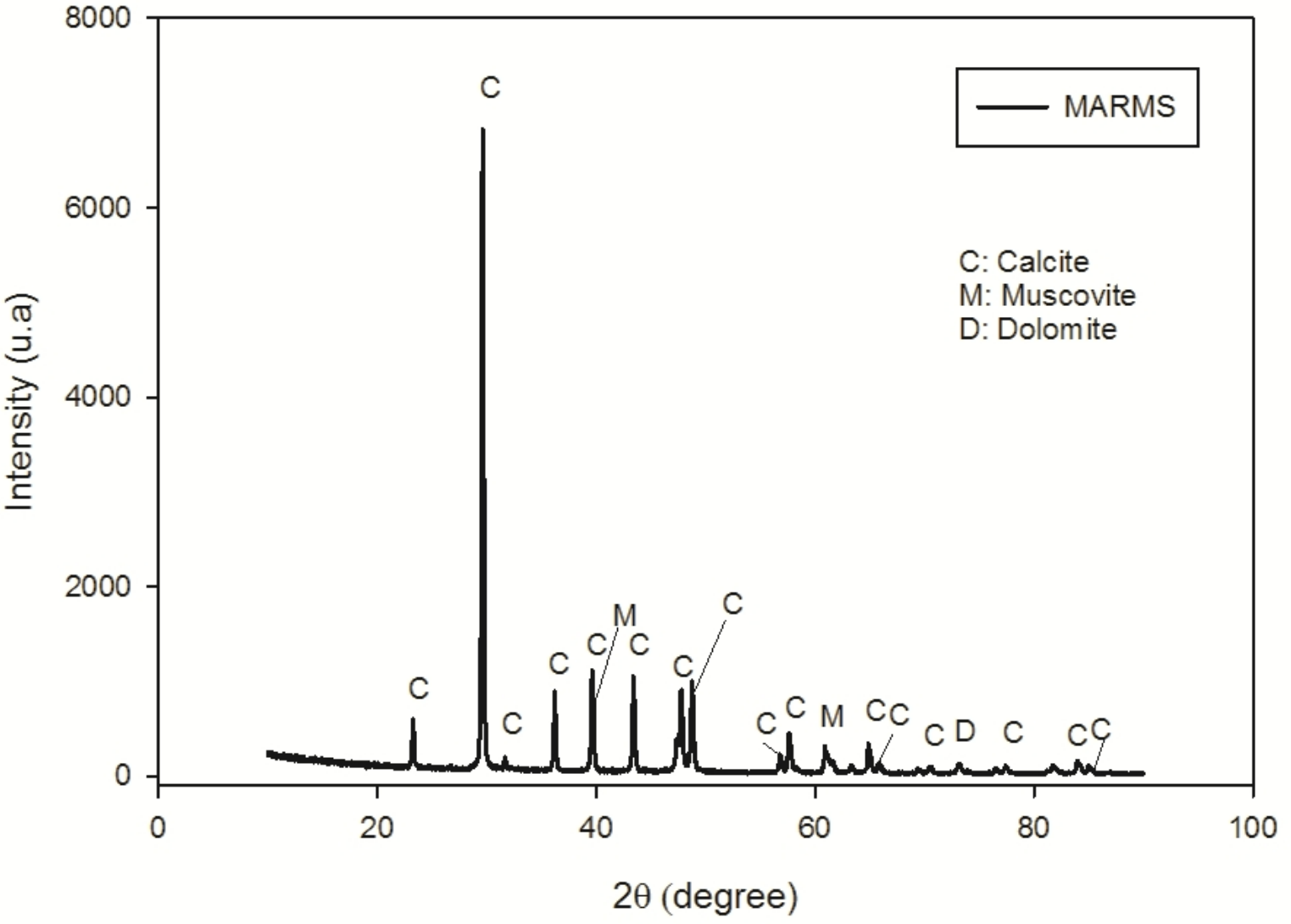
MARMS
C: Calcite
M: Muscovite
D: Dolomite
Intensity (u.a)
2θ (degree)
0
2000
4000
6000
8000
0
20
40
60
80
100
C
C
C
C
C
M
C
C
C
C
C
M
C
C
C
D
C
C
C

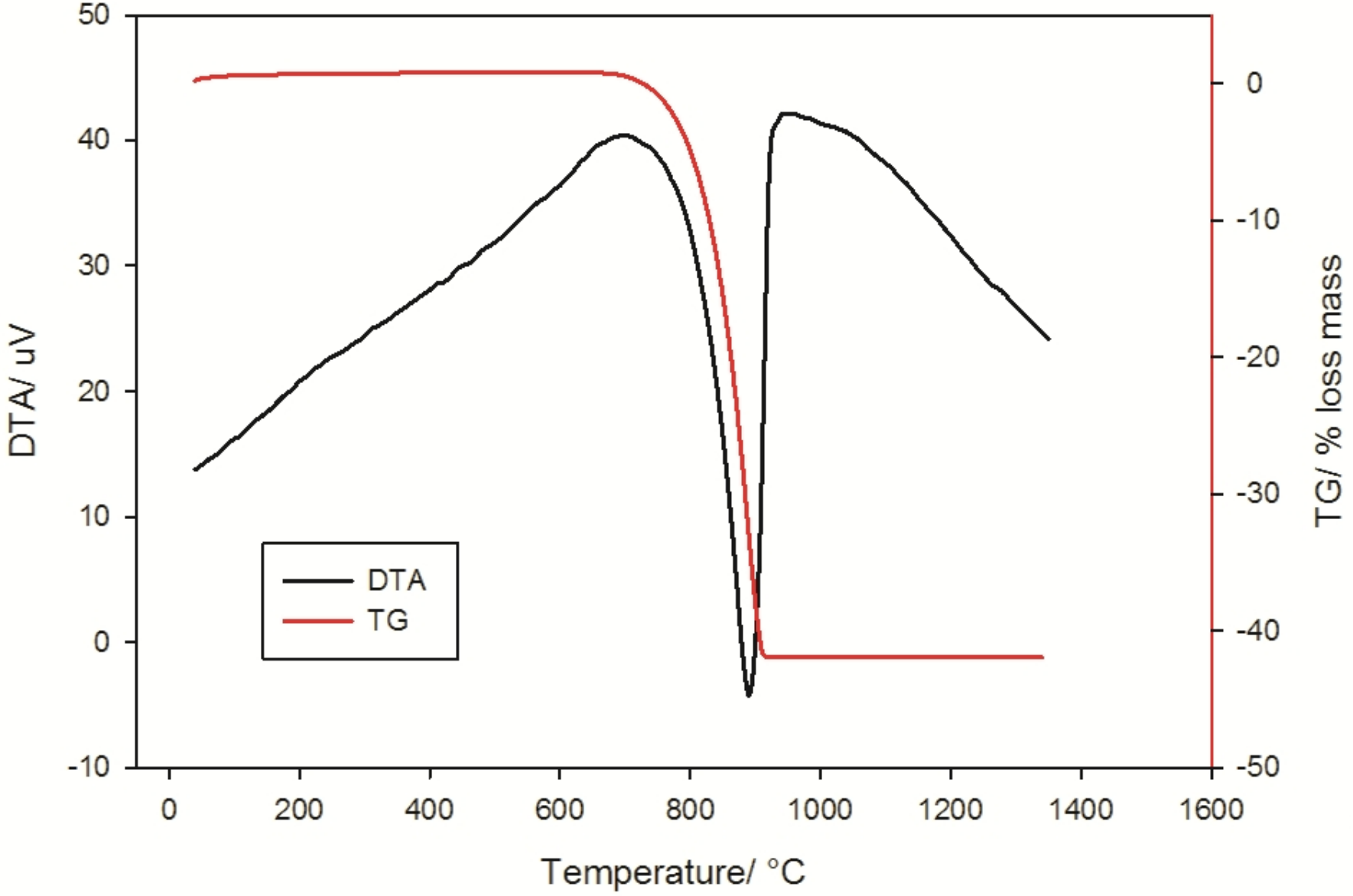
50
40
30
20
10
0
-10
DTA/ uV
0
-10
-20
-30
-40
-50
TG/ % loss mass
0
200
400
600
800
1000
1200
1400
1600
Temperature/ °C
DTA
TG

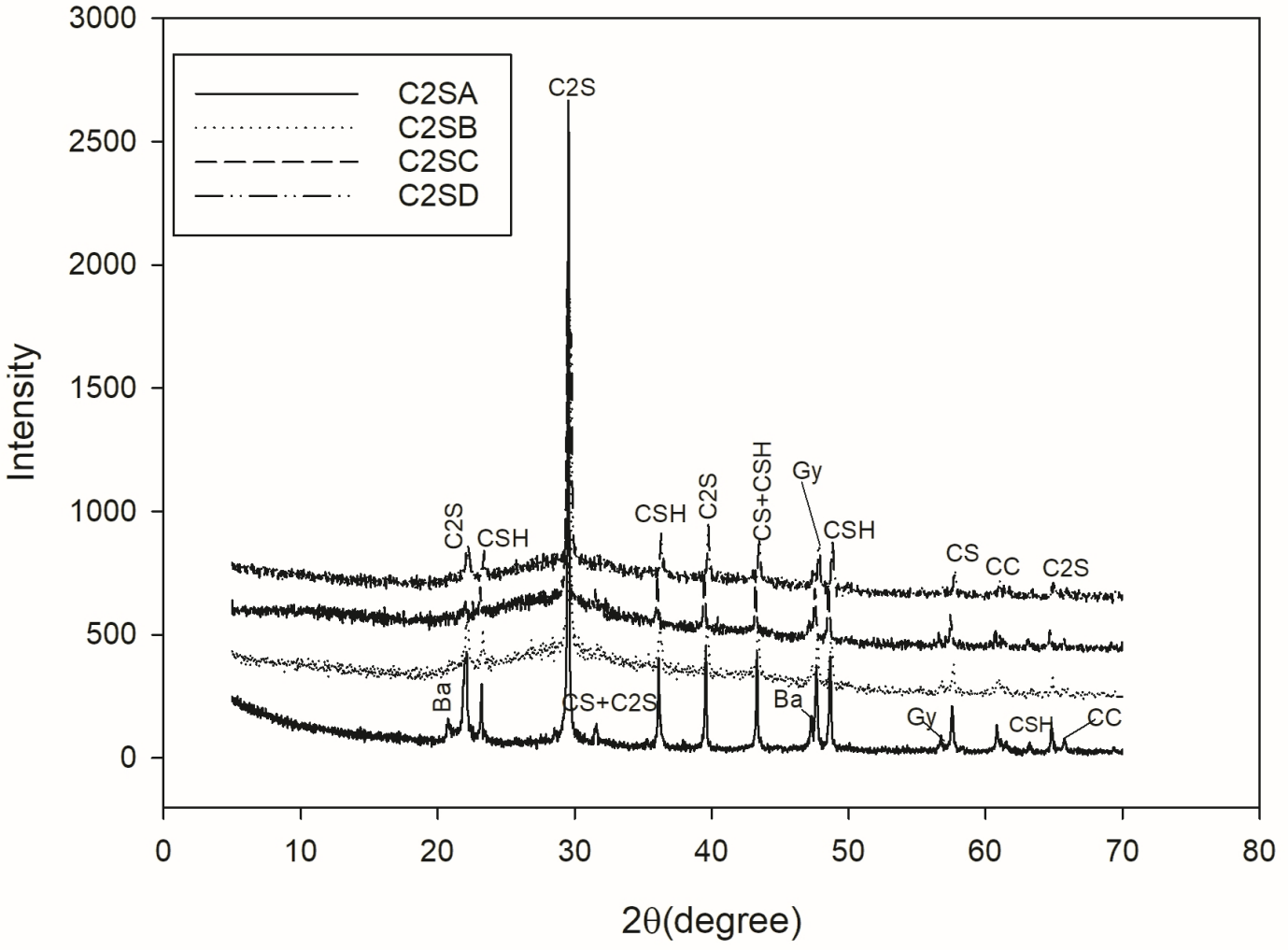

CSH: Calcium silicate hydrate, CS: Calcium silicate, Ba: Bassanite, C2S: Dicalcium silicate
Gy: Gypse, CC: Calcite

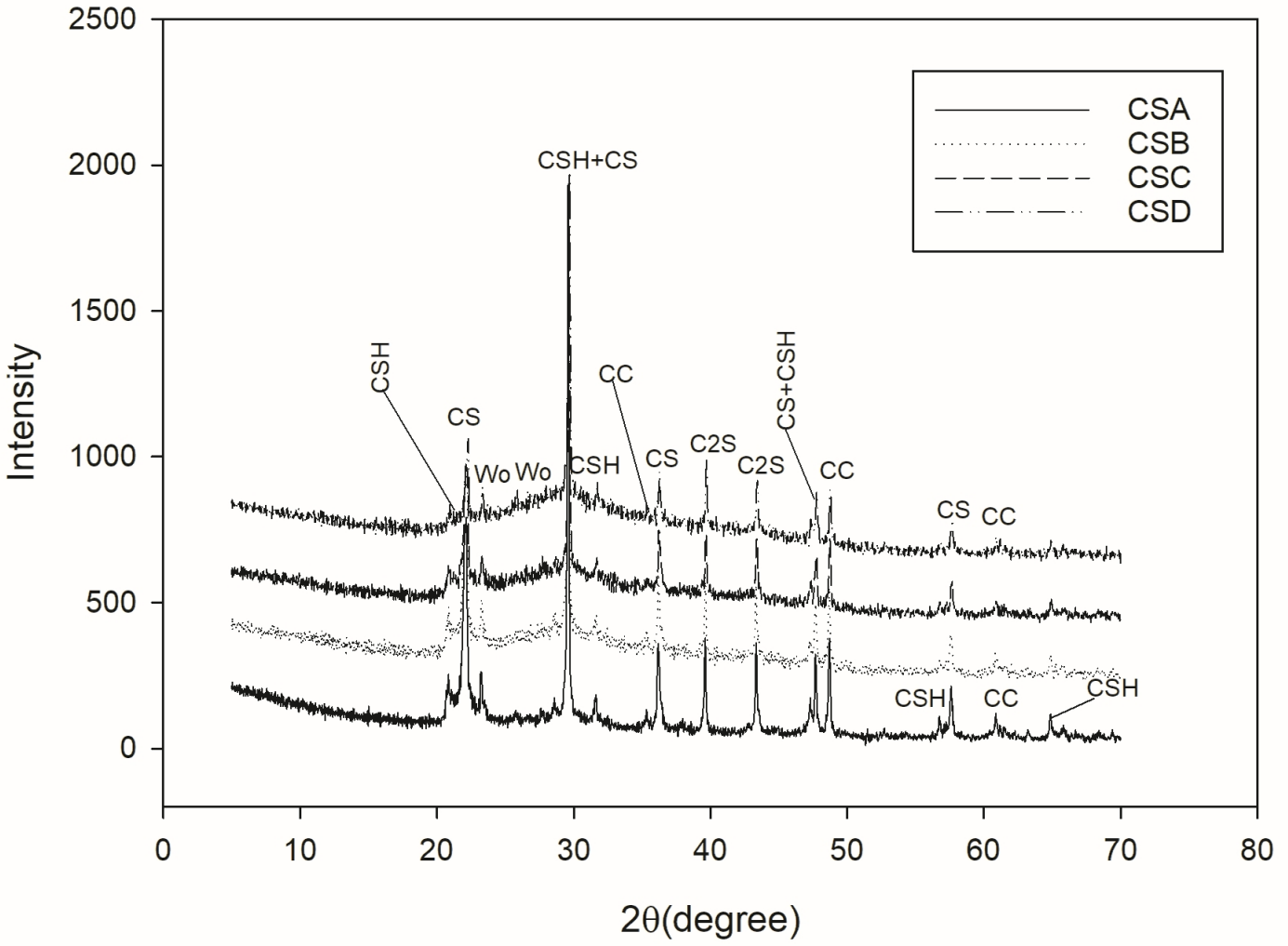

CSH: Calcium silicate hydrate, CS: Calcium silicate, Wo: Wollastonite, C2S: Dicalcium silicate
CC: Calcite

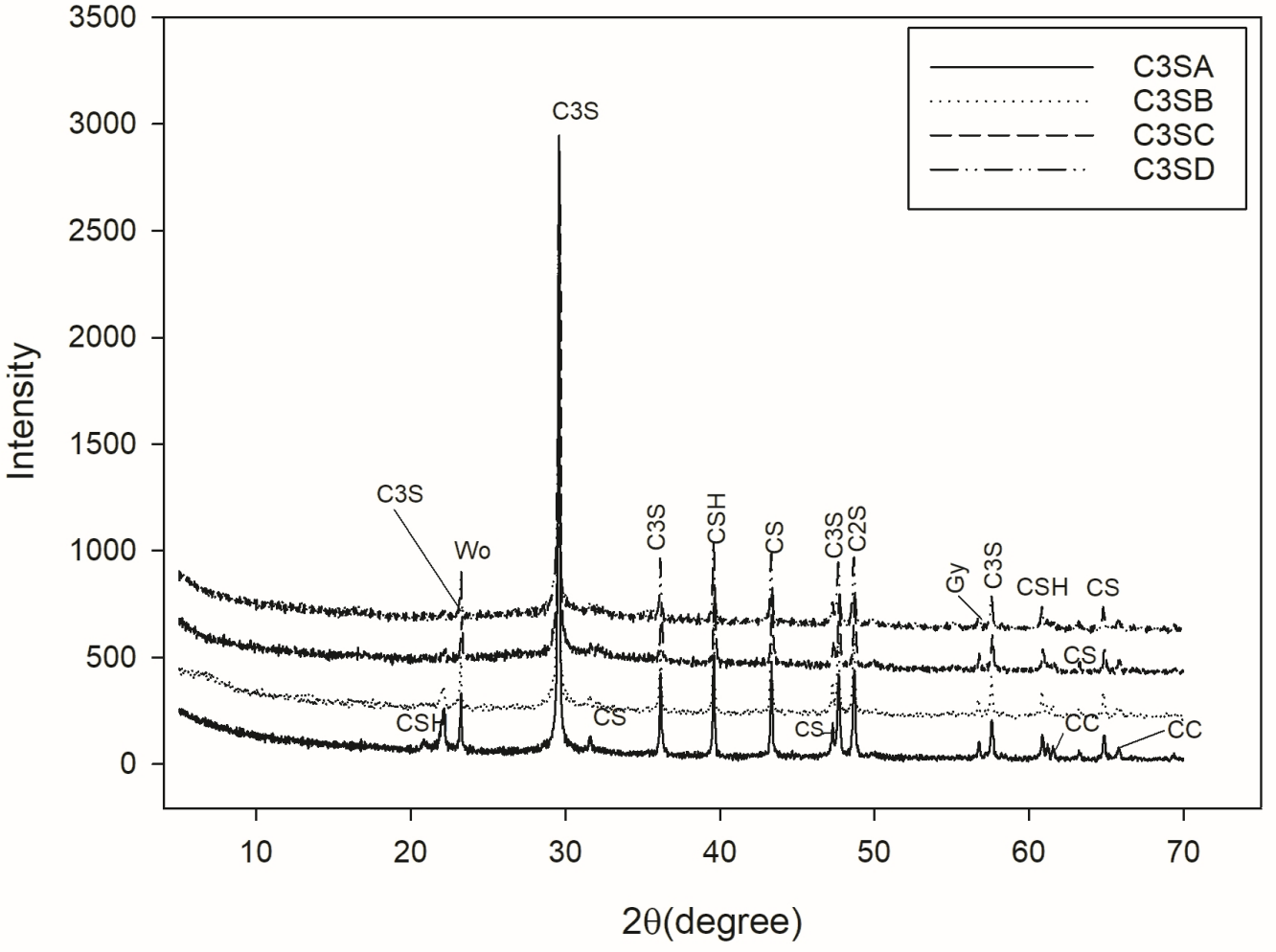

C3S: Tricalcium silicate, Wo: Wollastonite;CSH: Calcium silicate hydrate, CS: Calcium silicate,
C2S: Dicalcium silicate, Gy: Gypse, CC: Calcite

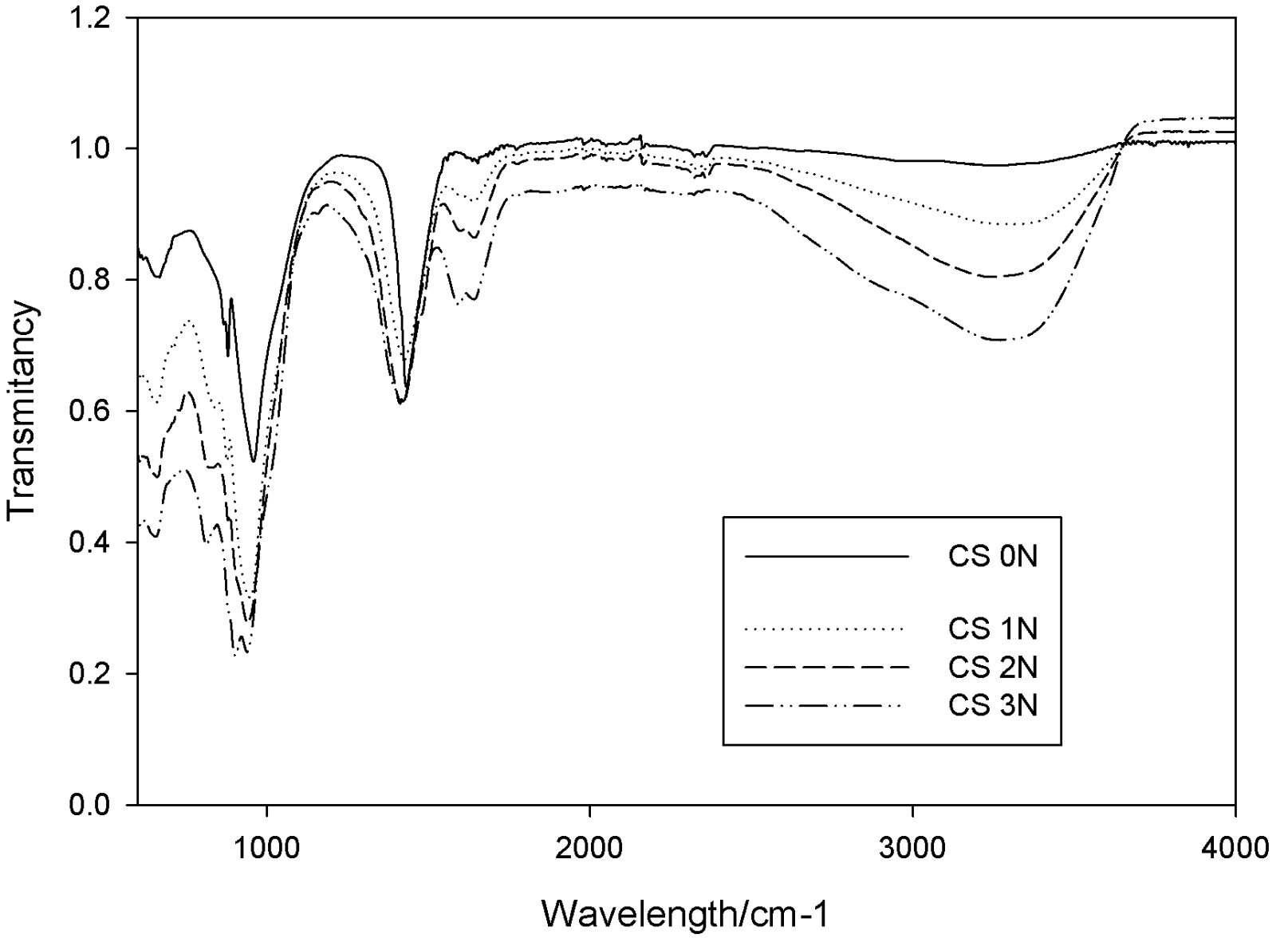
1.2
1.0
0.8
0.6
0.4
0.2
0.0
Transmitancy
1000
2000
3000
4000
Wavelength/cm-1
CS 0N
CS 1N
CS 2N
CS 3N

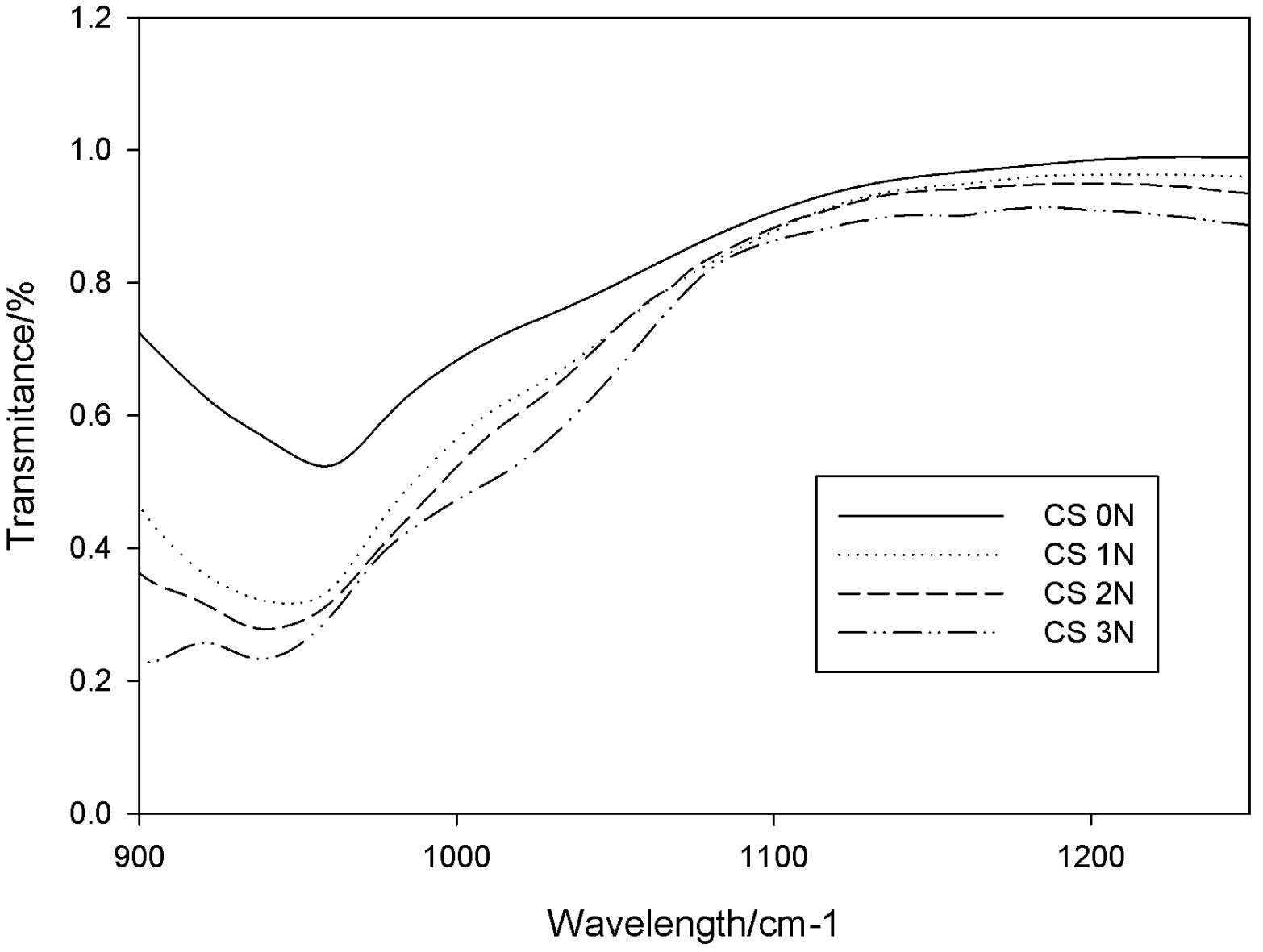
1.2
1.0
0.8
0.6
0.4
0.2
0.0
Transmitance/%
900
1000
1100
1200
Wavelength/cm-1
CS 0N
CS 1N
CS 2N
CS 3N

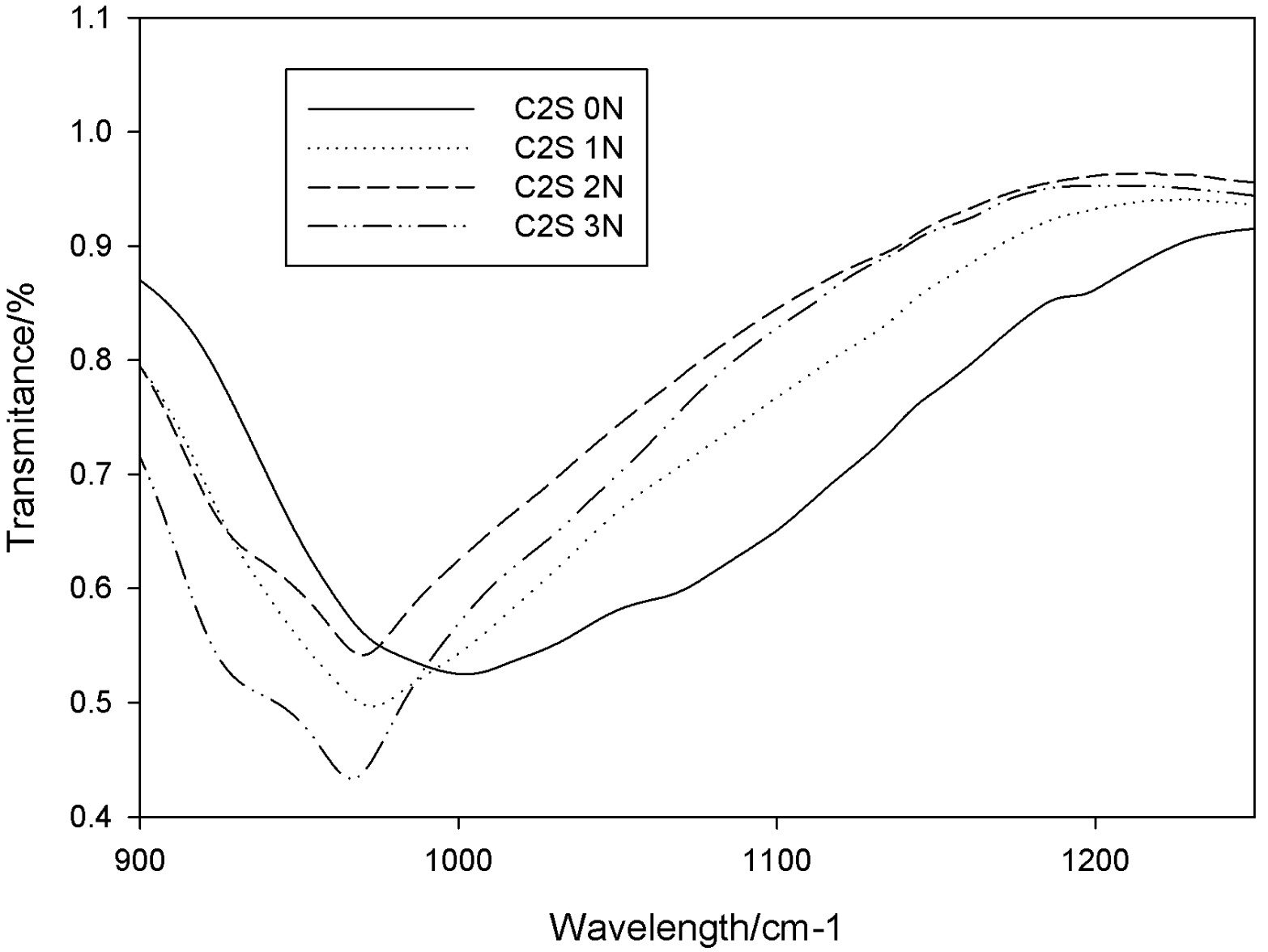
C2S 0N
C2S 1N
C2S 2N
C2S 3N
Transmitance/%
Wavelength/cm-1
1.1
1.0
0.9
0.8
0.7
0.6
0.5
0.4
900
1000
1100
1200

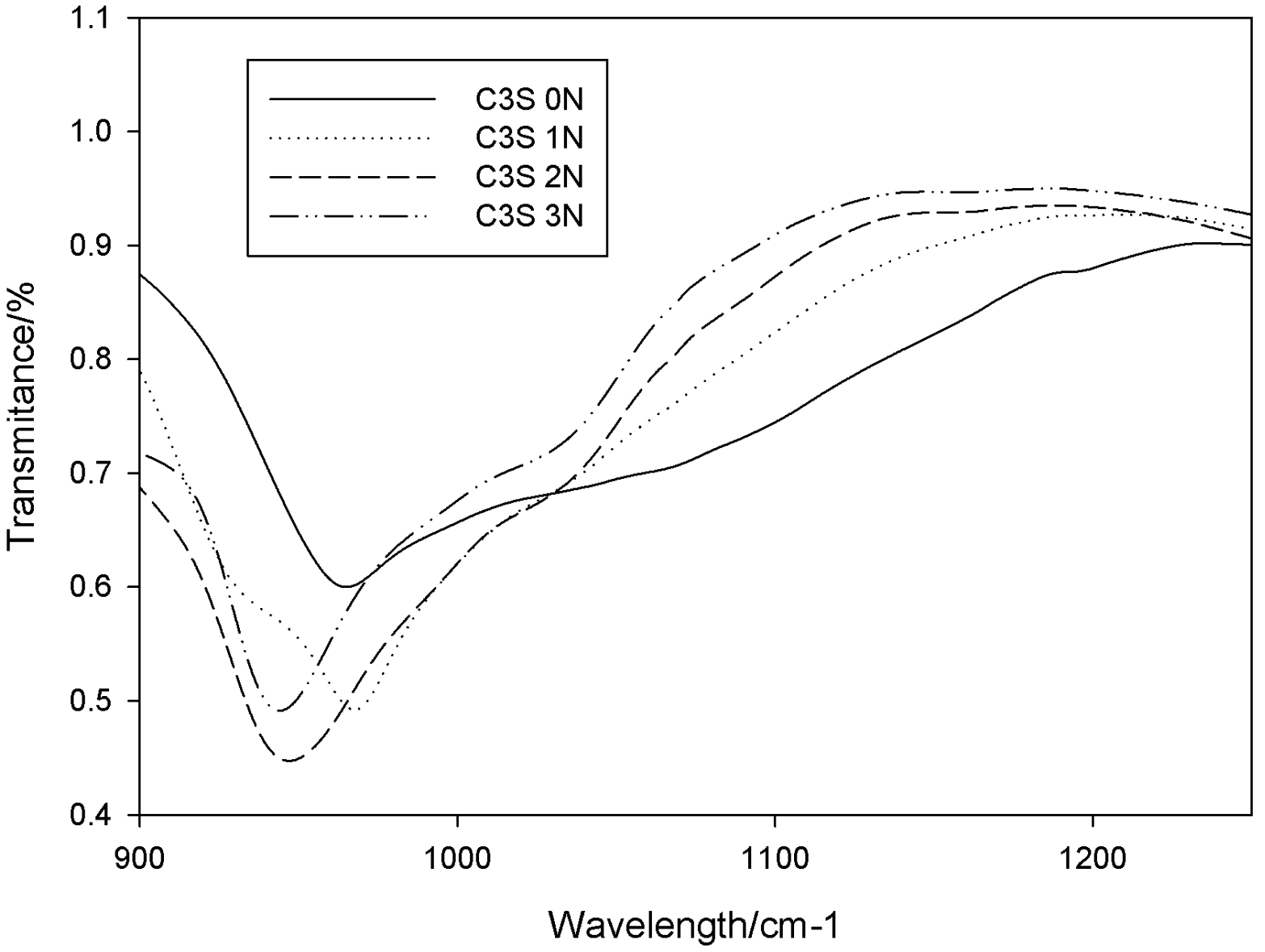
C3S 0N
C3S 1N
C3S 2N
C3S 3N
Transmitance/%
Wavelength/cm-1
1.1
1.0
0.9
0.8
0.7
0.6
0.5
0.4
900
1000
1100
1200

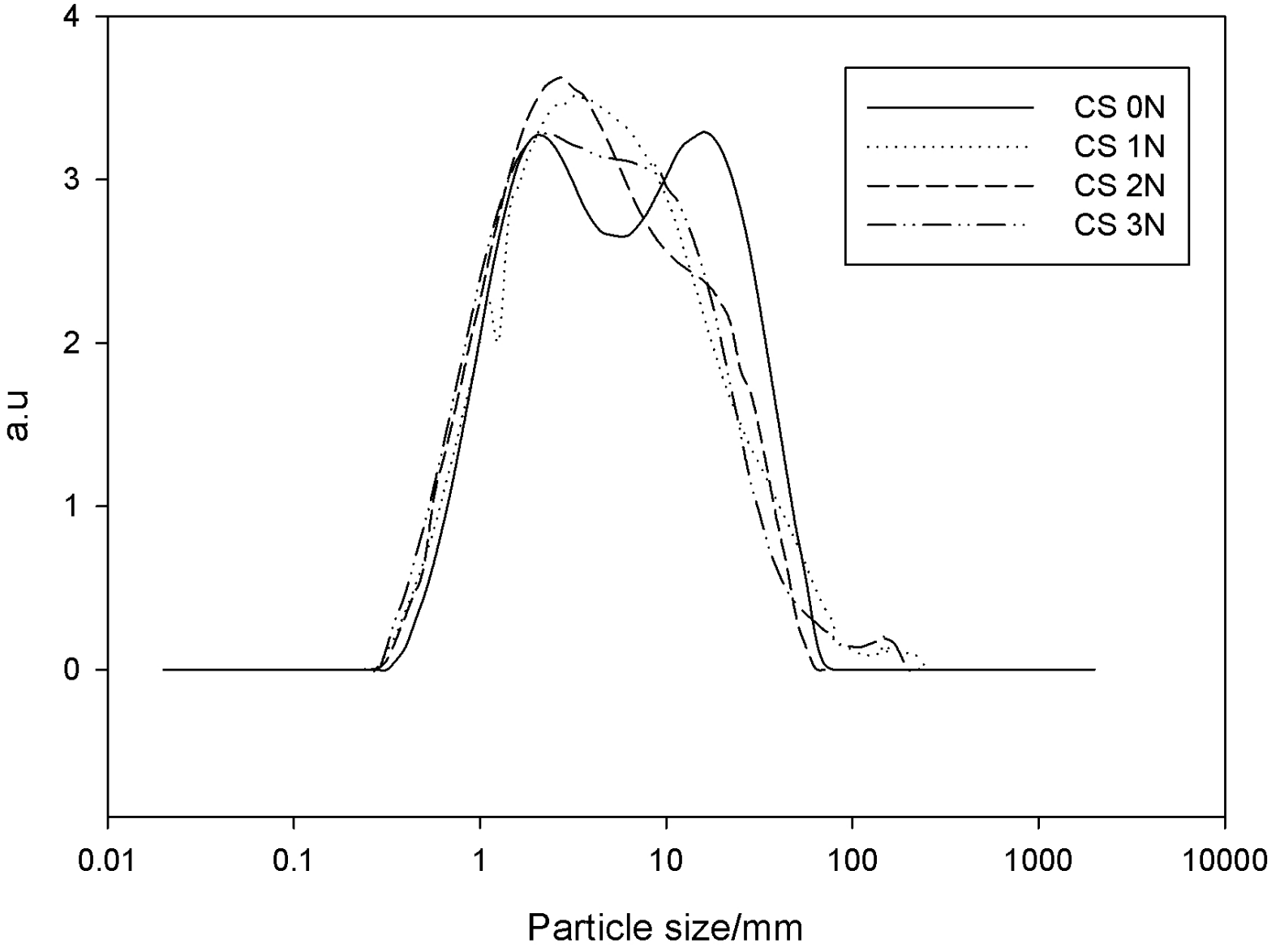
4
3
2
1
0
a.u
0.01
0.1
1
10
100
1000
10000
Particle size/mm
CS 0N
CS 1N
CS 2N
CS 3N

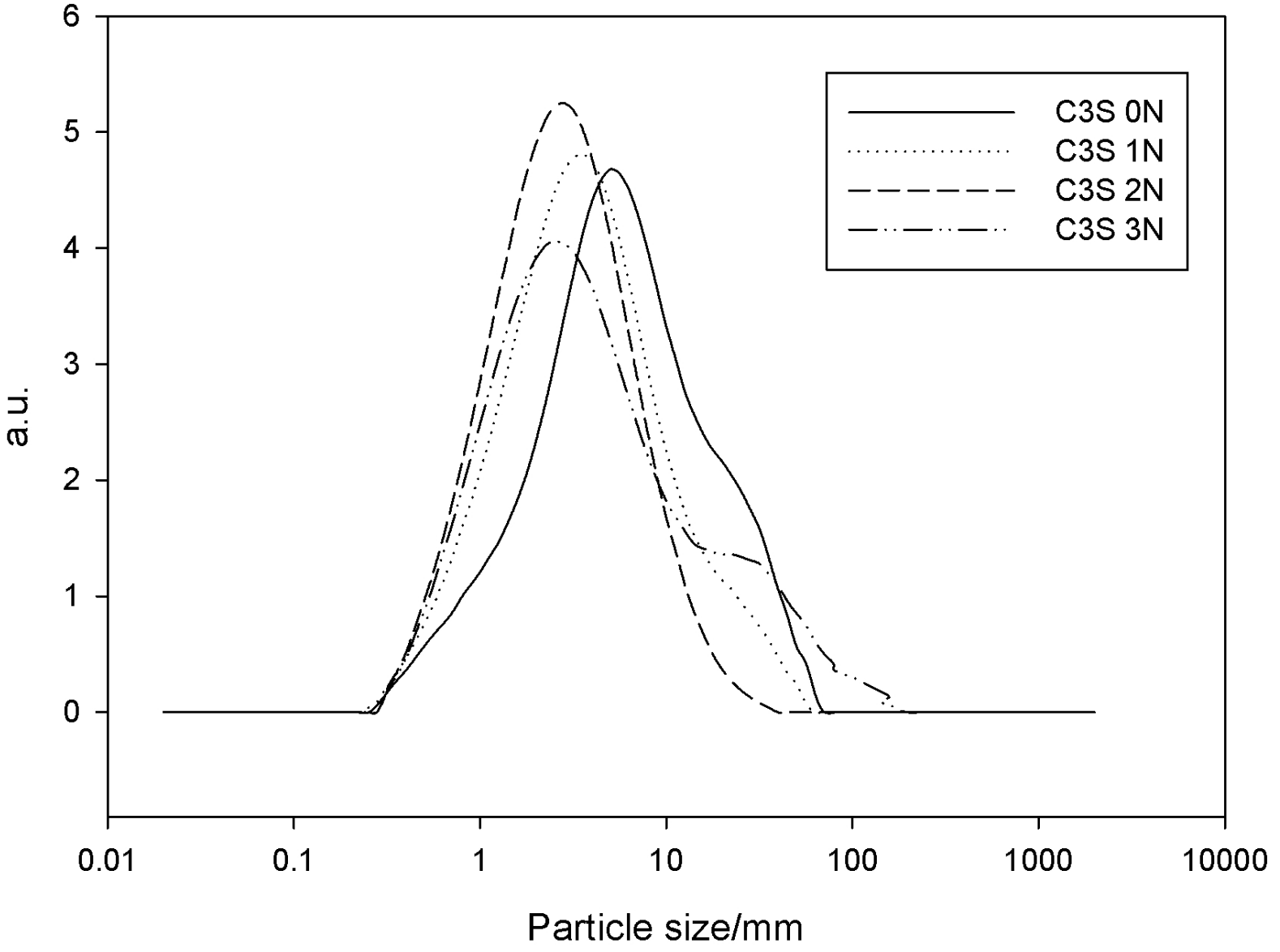
6
5
4
3
2
1
0
a.u.
0.01
0.1
1
10
100
1000
10000
Particle size/mm
C3S 0N
C3S 1N
C3S 2N
C3S 3N

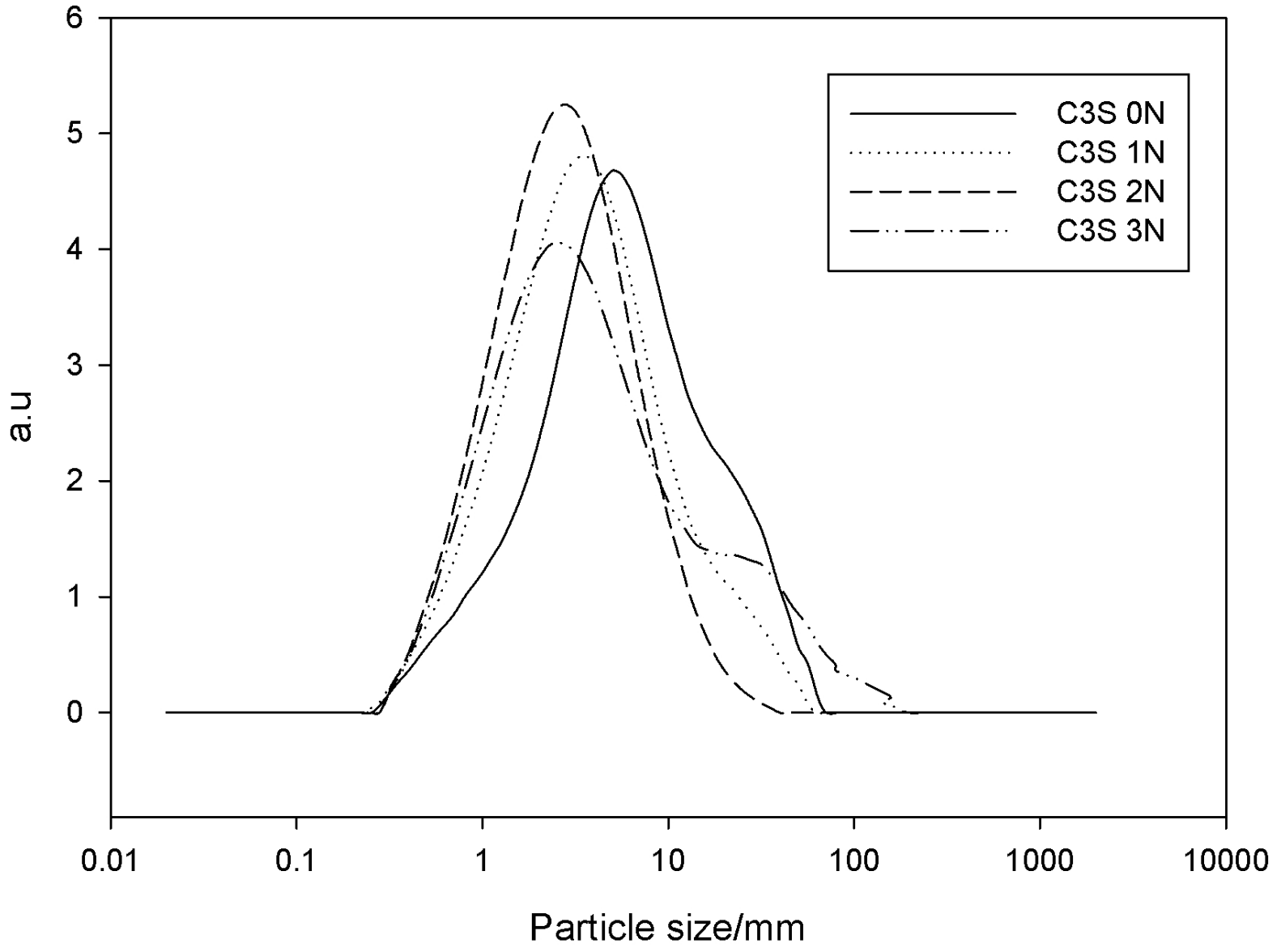
6
5
4
3
2
1
0
a.u
0.01
0.1
1
10
100
1000
10000
Particle size/mm
C3S 0N
C3S 1N
C3S 2N
C3S 3N

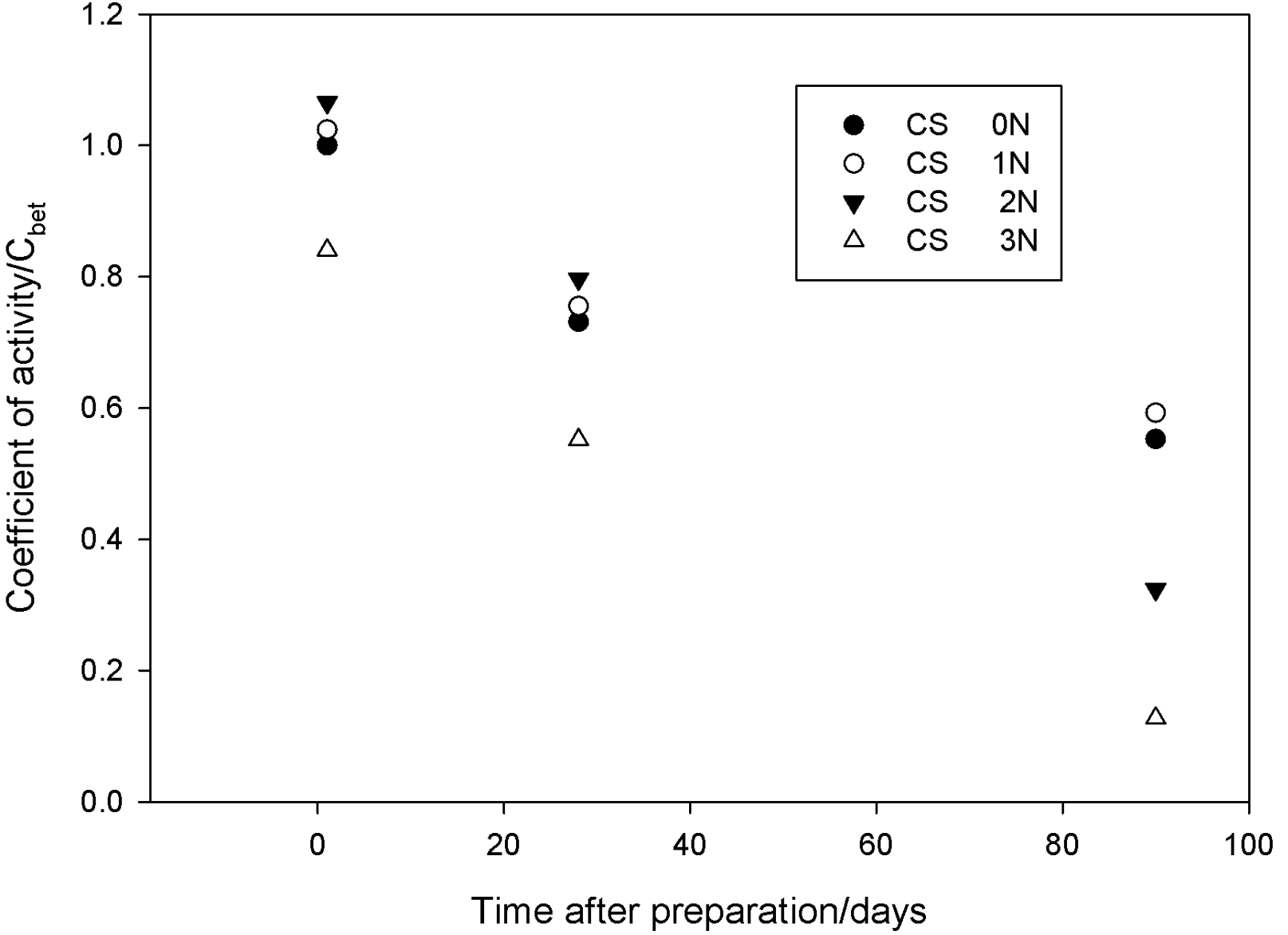
1.2
1.0
0.8
0.6
0.4
0.2
0.0
Coefficient of activity/C_{bet}
0
20
40
60
80
100
Time after preparation/days
CS 0N
CS 1N
CS 2N
CS 3N

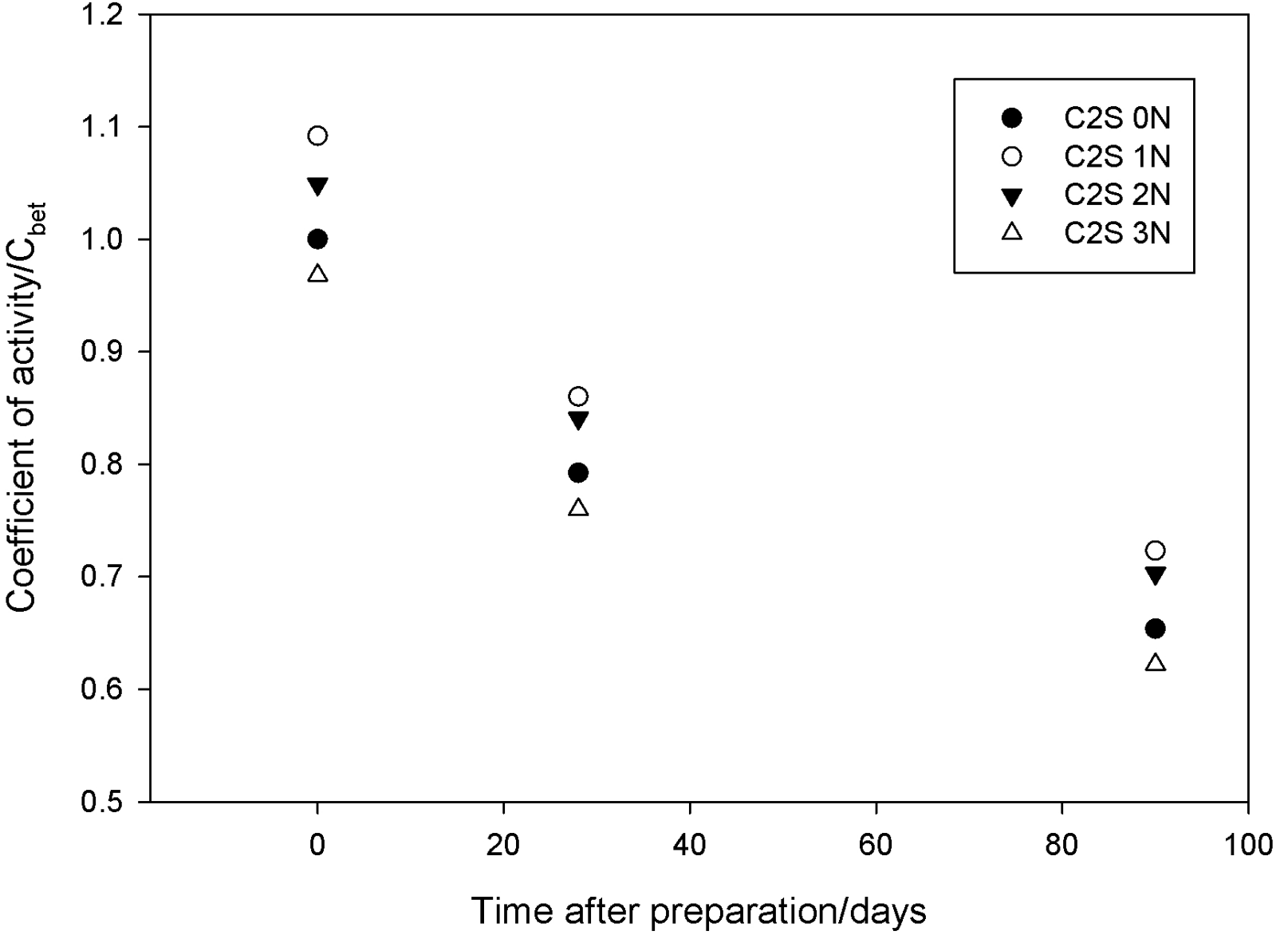
1.2
1.1
1.0
0.9
0.8
0.7
0.6
0.5
Coefficient of activity/C_{bet}
0
20
40
60
80
100
Time after preparation/days
C2S 0N
C2S 1N
C2S 2N
C2S 3N

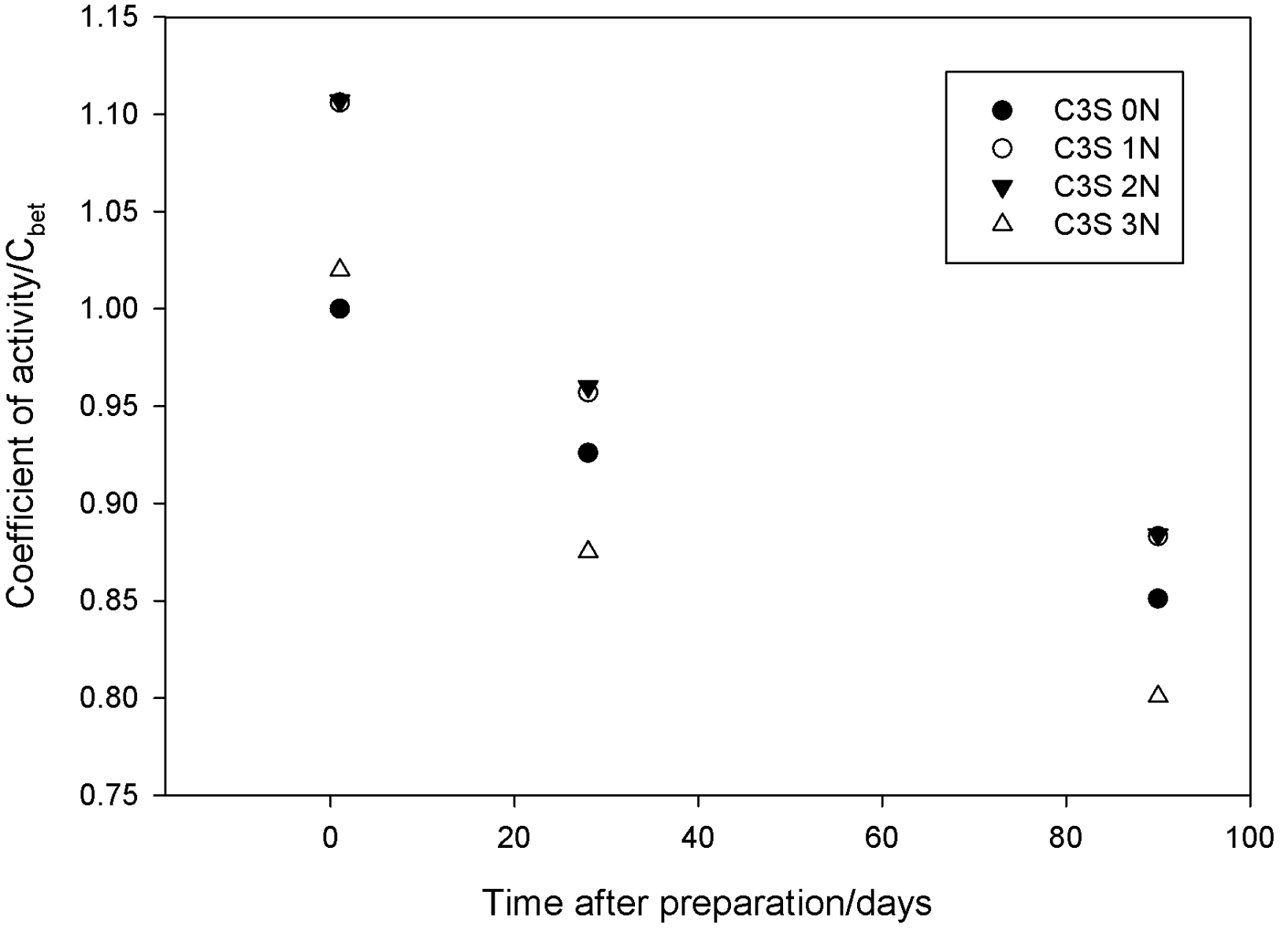
1.15
1.10
1.05
1.00
0.95
0.90
0.85
0.80
0.75
Coefficient of activity/C_{bet}
0
20
40
60
80
100
Time after preparation/days
C3S 0N
C3S 1N
C3S 2N
C3S 3N

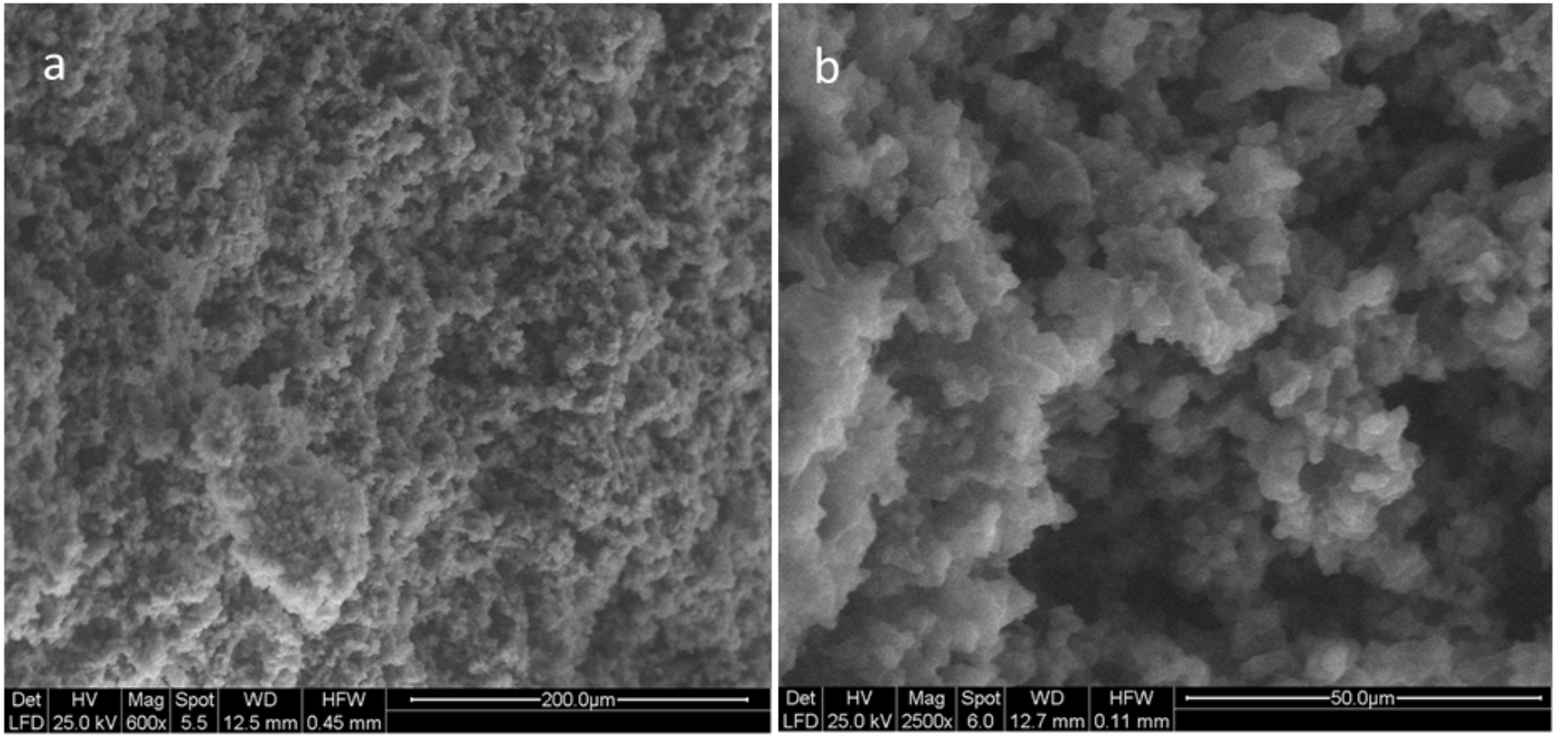
a
Det HV Mag Spot WD HFW
LFD 25.0 kV 600x 5.5 12.5 mm 0.45 mm
200.0µm
b
Det HV Mag Spot WD HFW
LFD 25.0 kV 2500x 6.0 12.7 mm 0.11 mm
50.0µm

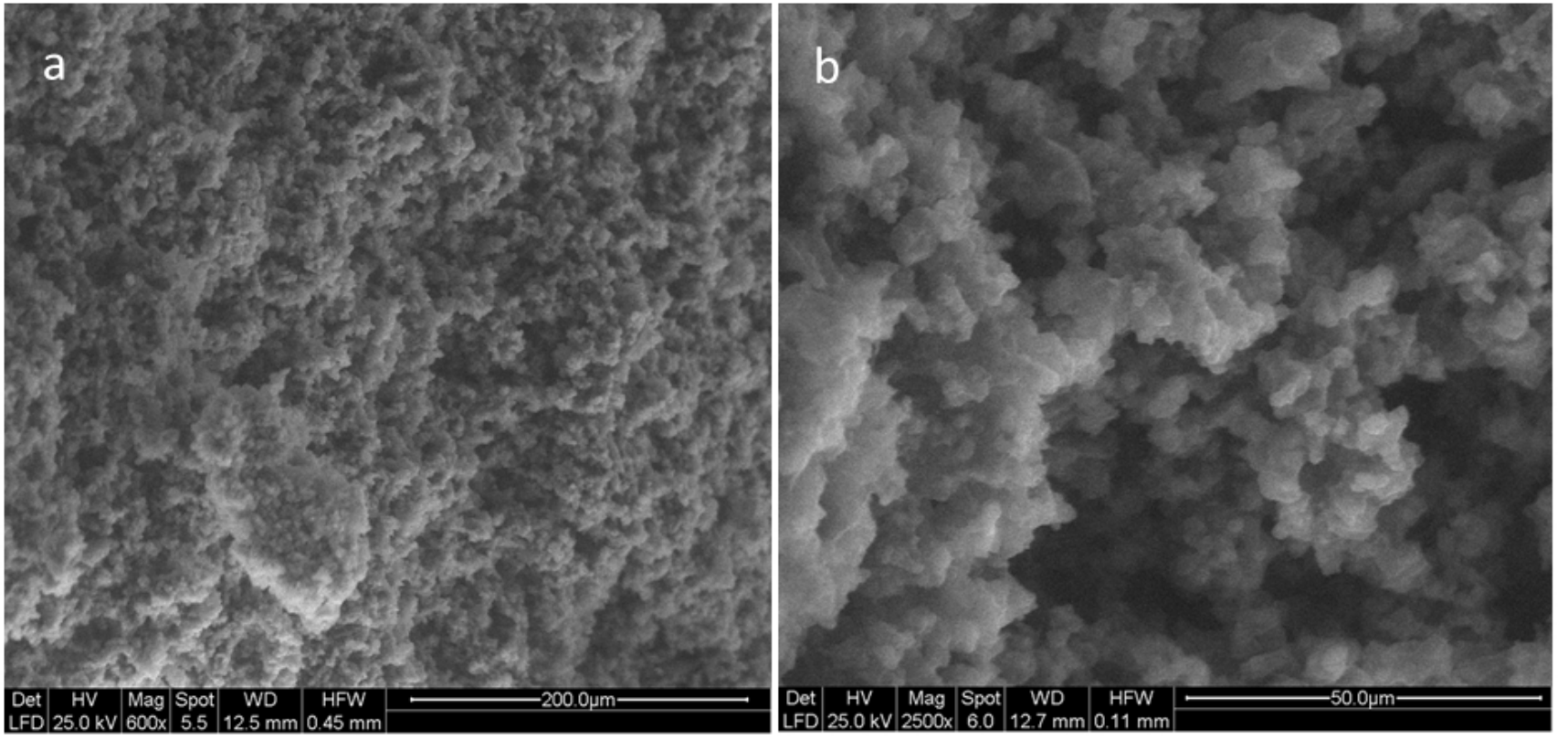
a
Det HV Mag Spot WD HFW
LFD 25.0 kV 600x 5.5 12.5 mm 0.45 mm
200.0µm
b
Det HV Mag Spot WD HFW
LFD 25.0 kV 2500x 6.0 12.7 mm 0.11 mm
50.0µm

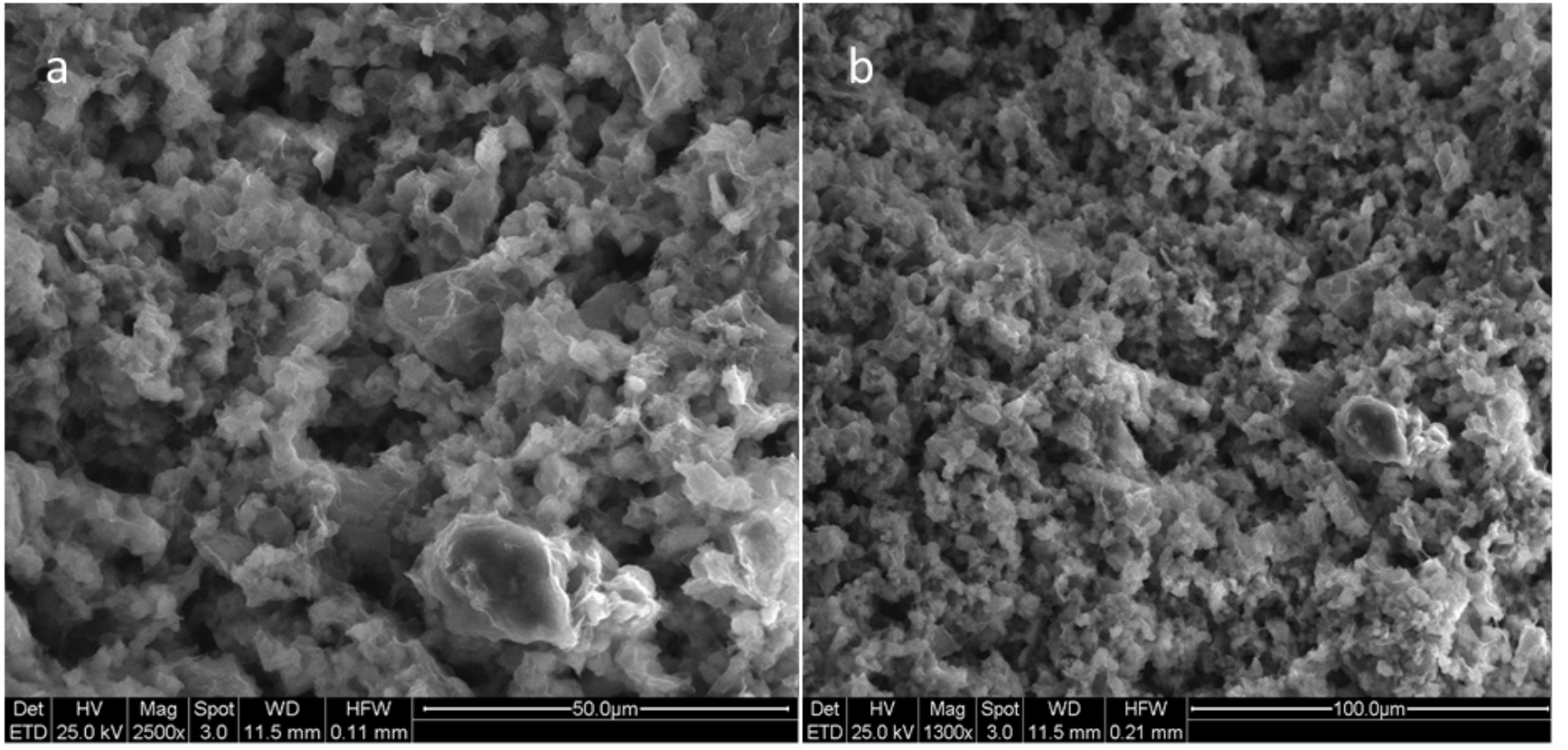
a
Det ETD
HV 25.0 kV
Mag 2500x
Spot 3.0
WD 11.5 mm
HFW 0.11 mm
50.0µm
b
Det ETD
HV 25.0 kV
Mag 1300x
Spot 3.0
WD 11.5 mm
HFW 0.21 mm
100.0µm

Table 1 :

Frequency (cm-1)	Assignment	Description
3270	H-OH	
1795	H bond	Stronger hydrogen bonds
1592	H-OH stretching	OH stretching associated with Si-OH and H_2O
938-960	Si-O-2NBO (Q^2)	O-Si-Ca_x + O-Si_2
898-920	Si-O-3NBO (Q^1)	O-Si-Ca_x and Si-O stretching
850-855	Si-O-4NBO (Q^0)	O-Si-Ca_x and Si-O stretching
810	S-O bending	Local structural disorder Silica chain depolymerization
654		Silica chain depolymerization